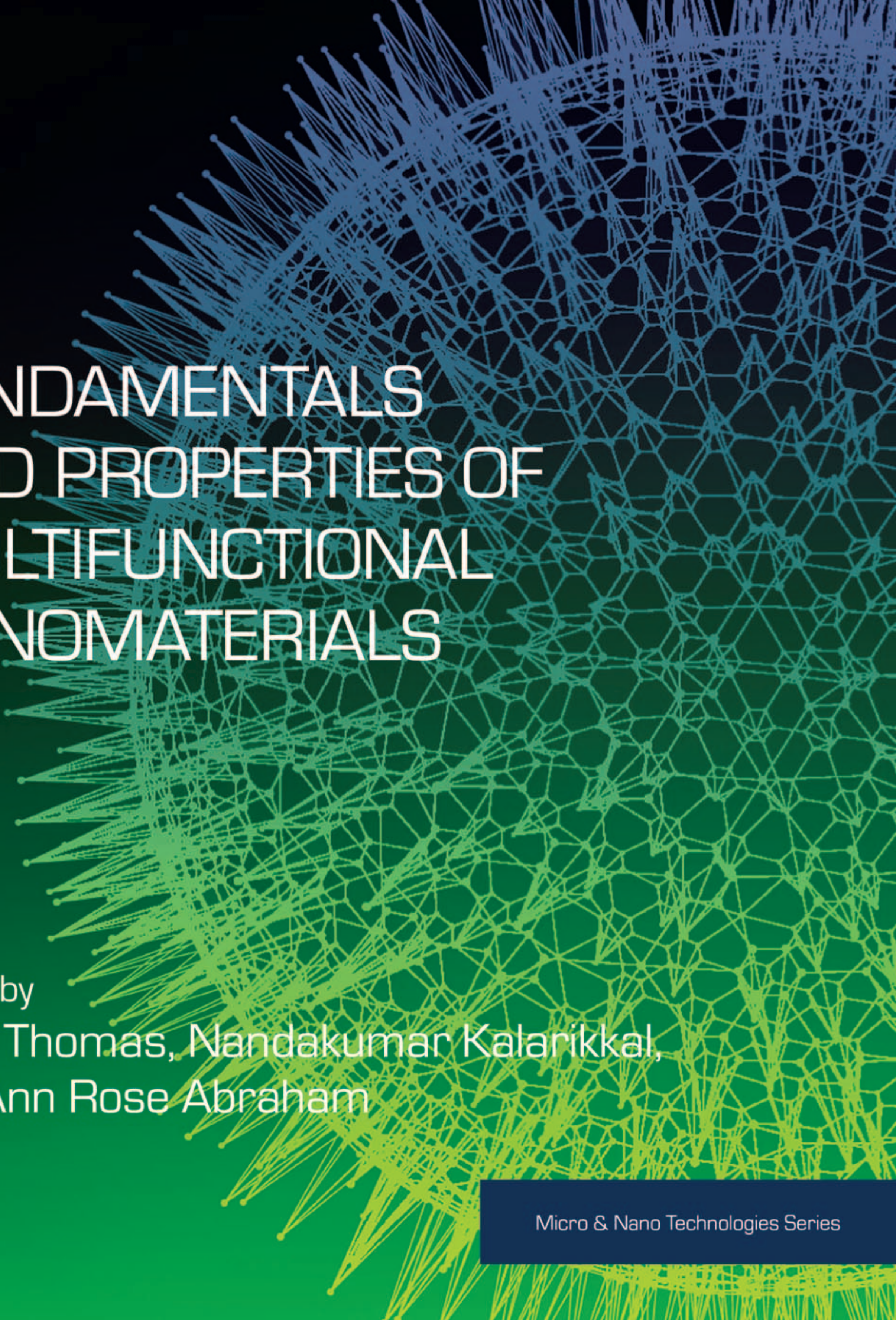

FUNDAMENTALS AND PROPERTIES OF MULTIFUNCTIONAL NANOMATERIALS

Edited by
Sabu Thomas, Nandakumar Kalarikkal,
and Ann Rose Abraham

ELSEVIER

Micro & Nano Technologies Series

Micro and Nano Technologies

Fundamentals and Properties of Multifunctional Nanomaterials

Edited by

Sabu Thomas

Nandakumar Kalarikkal

Ann Rose Abraham

ELSEVIER

Elsevier
Radarweg 29, PO Box 211, 1000 AE Amsterdam, Netherlands
The Boulevard, Langford Lane, Kidlington, Oxford OX5 1GB, United Kingdom
50 Hampshire Street, 5th Floor, Cambridge, MA 02139, United States

Copyright © 2021 Elsevier Inc. All rights reserved.

No part of this publication may be reproduced or transmitted in any form or by any means, electronic or mechanical, including photocopying, recording, or any information storage and retrieval system, without permission in writing from the publisher. Details on how to seek permission, further information about the Publisher's permissions policies and our arrangements with organizations such as the Copyright Clearance Center and the Copyright Licensing Agency, can be found at our website: www.elsevier.com/permissions.

This book and the individual contributions contained in it are protected under copyright by the Publisher (other than as may be noted herein).

Notices

Knowledge and best practice in this field are constantly changing. As new research and experience broaden our understanding, changes in research methods, professional practices, or medical treatment may become necessary.

Practitioners and researchers must always rely on their own experience and knowledge in evaluating and using any information, methods, compounds, or experiments described herein. In using such information or methods they should be mindful of their own safety and the safety of others, including parties for whom they have a professional responsibility.

To the fullest extent of the law, neither the Publisher nor the authors, contributors, or editors, assume any liability for any injury and/or damage to persons or property as a matter of products liability, negligence or otherwise, or from any use or operation of any methods, products, instructions, or ideas contained in the material herein.

Library of Congress Cataloging-in-Publication Data
A catalog record for this book is available from the Library of Congress

British Library Cataloguing-in-Publication Data
A catalogue record for this book is available from the British Library

ISBN: 978-0-12-822352-9

For information on all Elsevier publications visit our website at
https://www.elsevier.com/books-and-journals

Publisher: Matthew Deans
Acquisitions Editor: Simon Holt
Editorial Project Manager: Chiara Giglio
Production Project Manager: Sojan P. Pazhayattil
Cover Designer: Christian J. Bilbow

Typeset by TNQ Technologies

ELSEVIER
Book Aid International
Working together to grow libraries in developing countries
www.elsevier.com • www.bookaid.org

Contents

PART 1: Nanoscopic solids and transport properties

PART 2: Properties of liquid crystalline nanomaterials

PART 3: Properties of carbon-based nanomaterials

PART 4: Characteristics of magnetic nanomaterials

PART 6: Properties of plasmonic nanomaterials

PART 7: Engineered nanomaterials for industrial applications

PART 8: Fundamentals of 2D nanomaterials

PART 9: The impact of nanomaterials on health and safety

CHAPTER 13

Multifunctional plasmonic nanomaterials

Sudhir Cherukulappurath
School of Physical and Applied Sciences, Goa University Taleigao Plateau, Goa, India

Chapter Outline

1. Introduction

Recent progress in synthesis methods of nanomaterials has enabled the development of novel structures with multifunctional properties. By proper engineering, it is now possible to have the desired character for the nanomaterial for specific applications. In this regard, plasmonic nanoparticles have been one of the most researched materials in recent decade owing to their potential applications in different areas. It is now possible to manipulate light to sub-diffraction level by harnessing the surface conduction electron excitations of metals, called surface plasmons that are coupled to electromagnetic waves. While plasmonic nanoparticles by themselves have proven to be useful in a broad range of applications such as biomedical technology, sensing, and nanoscale optoelectronic devices, a recent trend has been to add additional features to the plasmonic nanoparticles to make them multifunctional. For example, a nanoparticle with a magnetic core and plasmonic shell will have diverse applications in biomedical imaging and photothermal treatments.

Fundamentals and Properties of Multifunctional Nanomaterials. https://doi.org/10.1016/B978-0-12-822352-9.00002-X

By combining a fluorescent material such as semiconductor quantum dots with plasmonic nanoparticles, it is possible not only to broaden the scope of the nanomaterials but also to observe interesting physical processes such as fluorescence enhancement and quenching.

This chapter will review some of the basic geometries of multifunctional plasmonic nanoparticles and their applications. The first part of the chapter is an introduction to plasmonic materials where in the concept of surface plasmons will be introduced. The second part will consist of a description of the common multifunctional plasmonic nanoparticles such as plasmonic core-magnetic shell nanoparticles, magnetic core-plasmonic shell nanoparticles, and fluorescent plasmonic nanoparticles. The graphene-plasmonic nanoparticle nanocomposites will be discussed in the subsequent section.

2. Plasmonic nanoparticles: theory, synthesis, and properties

The science of scattering of light has fascinated mankind since long time. In particular, scattering by colloidal particles has been studied for their interesting optical properties. Gold and silver colloids were probably one of the earliest materials in nano-size that were of great interest in the beginning of the 20th century. Zsigmondy had studied and characterized colloidal gold solutions using an ultramicroscope [1]. Several theoretical explanations including those from Maxwell Garnet, Lorentz, Debye, and Mie were developed to support the experimental observation of absorption and scattering peaks of colloidal gold solutions. In 1902, R. W. Wood had reported certain uneven distribution of light after diffraction from reflection gratings [2]. It was also observed that this distribution was strongly polarization dependent. An explanation to these “Wood’s Anomalies” was given by Lord Rayleigh [3] and later by Fano [4] based on surface waves. It was in 1957, when Ritchie reported the connection between the electron excitation in metal films and the surface waves which led to a whole new branch called plasmon optics or plasmonics [5]. Ritchie’s explanations were based on the electron energy absorption by metallic films by the generation of surface waves were termed surface plasmons. Two years after, the existence of plasma oscillations was confirmed experimentally using electron energy loss experiments by Powell and Swan [6]. Later, the quanta of these plasma excitations were termed surface plasmons by Stern and Ferrell [7]. This led to the generation of a whole new field of research in condensed matter physics which grew exponentially not only because of the interesting physics involved but also owing to its potential in several novel applications. The study, generation, and manipulation of surface plasmons for engineered light-matter interaction at the nanoscale developed into a new branch termed ’plasmonics’, just as electronics for the harness of electrons and photonics for photons [8,9]. There has been a clear distinction between two types of surface plasmons: surface plasmon polaritons (SPPs) is generally a term reserved for the propagating conduction electron excitations along a metal-dielectric interface and localized surface plasmons (LSPs) are non-propagating charge density oscillations excited by electromagnetic waves on the surface of metallic nanostructures [10].

SPPs are basically two-dimensional surface waves that can propagate along the interface of a metal and dielectric (Fig. 13.1A) [11,12]. The confinement of SPPs to the surface leads to strong sensitivity to the surface conditions such as the refractive index of the dielectric medium that has been exploited in several sensing platforms such as biosensing and chemical sensing [13–17]. This enhanced sensitivity has also led to other interesting processes such as surface-enhanced Raman scattering (SERS) and fluorescence, second harmonic generation and extraordinary transmission through apertures and films.

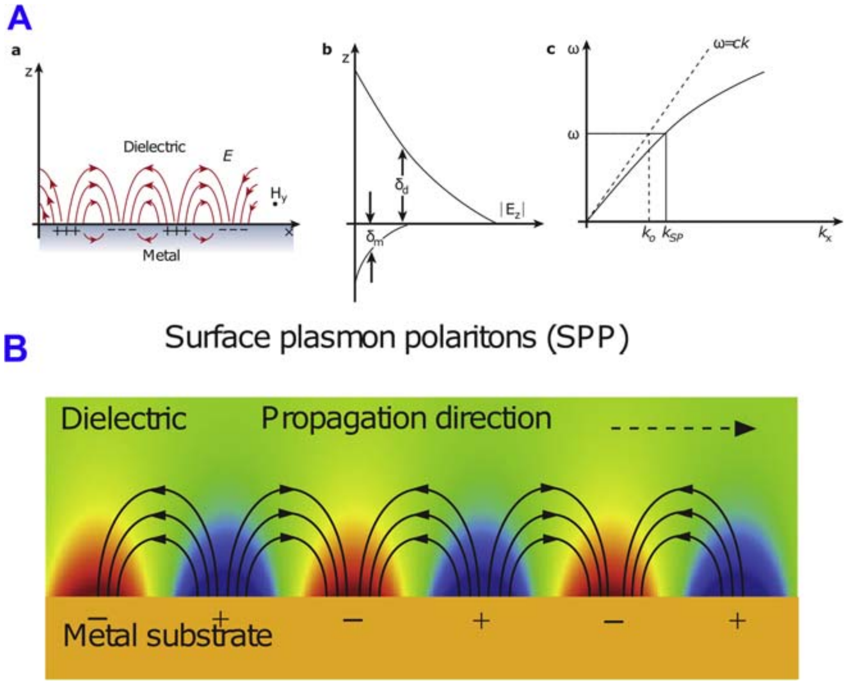

Figure 13.1

(A) Surface Plasmon Polaritons (a) Propagation of surface plasmon polariton (SPP) at the metal-dielectric interface. (b) SPPs are evanescent in the z-direction (toward the metal and medium) such that there is an exponential decay of energy. The decay length into the metal is determined by its skin depth. (c) Typical dispersion curve of SPP which is always lying below the light line. This means that it is not possible to directly excite SPPs. (B) Electromagnetic field distribution of surface plasmons at the interface. *(C) Reprinted with permission from Barnes, W. L.; Dereux, A.; Ebbesen, T. W. Surface plasmon subwavelength optics. Nature 2003, 424 (6950), 824–830. https://doi.org/10.1038/nature01937; (D) Reprinted with permission from Davis, T. J.; Gómez, D. E.; Roberts, A. Plasmonic circuits for manipulating optical information. nanophotonics 2016, 6 (3), 543–559. https://doi.org/https://doi.org/10.1515/nanoph-2016-0131.*

The theory of SPP generation and propagation has been well-studied, and there are several resourceful references on this subject [10,18–22]. The Drude theory of metals can be used as an approximation to understand the properties of metals and their interaction with light. Based on this theory, it has been shown that for exciting SPPs at the metal-dielectric interface, the real part of the dielectric function of the metal should be less than or equal to zero [18]. This implies that surface plasmons can exist only at the interface of materials that have opposite signs of the dielectric function. Noble metals such as gold and silver easily satisfy this condition in the UV-visible frequencies. It has also been established that these surfaces can exist only for certain polarization (transverse-magnetic or TM mode). The dispersion relation of SPP propagating along the interface of a Drude metal and a dielectric is given by [11]:

$$k_{SP} = k_0 \sqrt{\frac{\varepsilon_d \varepsilon_m}{\varepsilon_d + \varepsilon_m}}$$

where $\hbar k_{SP}$ denotes the momentum of the propagating surface plasmons in the metal-dielectric interface, while k_0 is the propagation constant of light in vacuum. ε_d and ε_m are the frequency-dependent permittivity of the dielectric medium and the metal. For sustaining surface plasmons on the interface, the two permitivities should be of opposite sign. Hence noble metals such as gold and silver are preferred as plasmonic metals in the visible region of electromagnetic spectrum. The SPP fields are evanescent, which means that in the perpendicular directions, the field intensity decay exponentially (see Fig. 13.1B).

It may be observed that the dispersion plot of SPP propagation lies on the right of the light line for air or silica (see Fig. 13.1C). This implies that the momentum of surface plasmons is larger that of a free photon or photons in silica. Thus, to excite the SPPs, additional momentum needs to be supplied, which often is called the phase matching condition. There are several methods to impart the extra momentum to excite the SPPs. The most common ones include using the evanescent fields of light under total internal reflection (also called as Kretschmann configuration), tight focusing configurations, and using grating structures.

On the other hand, LSPs are nonpropagating conduction electron excitations in metal nanoparticles that are coupled to electromagnetic field [10]. These field oscillations impart interesting optical properties to the metal nanoparticles such as tunable color of the scattered/absorbed light, and the generation of enhanced local electromagnetic field. LSP modes arise from the scattering nature of subwavelength particles that are subjected to an oscillating electromagnetic field. Unlike SPPs, the curvature of the surface of the nanoparticles results in an effective restoring force on these oscillating conduction electrons that can attain a resonant condition leading to the enhancement of the local field at resonance (Fig. 13.2A). This LSP resonance, usually called LSPR, is often used in

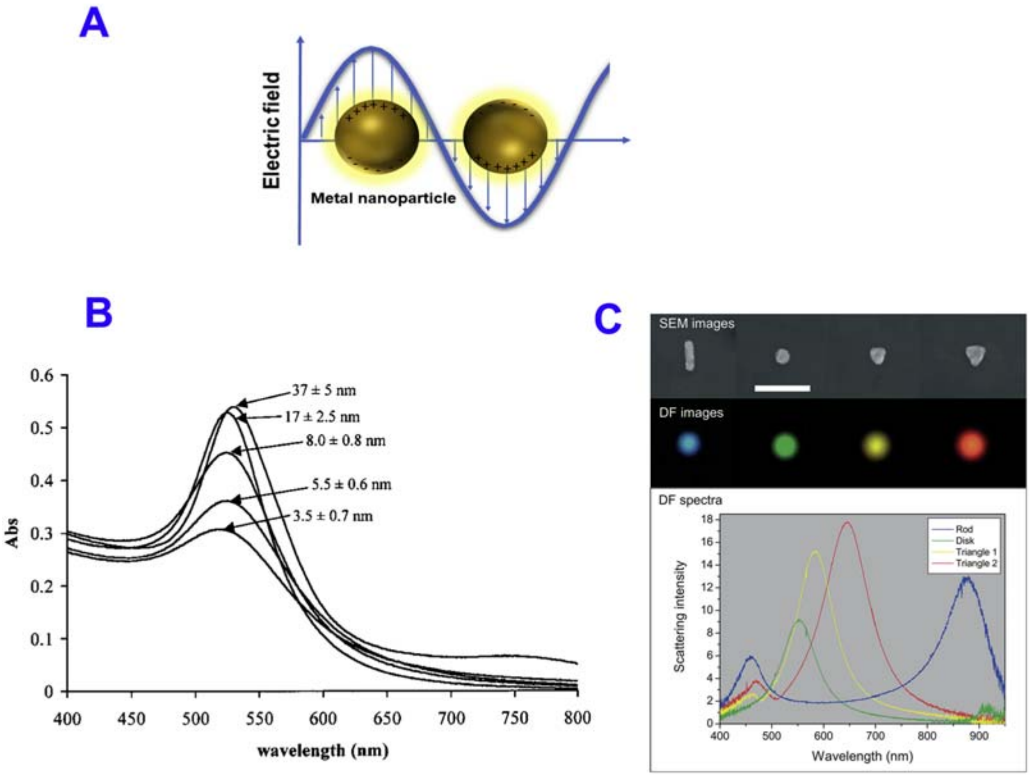

Figure 13.2

(A) Localized surface plasmon excitations in metal nanoparticles are nonpropagating. Delocalized surface electrons oscillate along with the external electric field resulting in an enhanced local field. (B) Absorption spectra of gold nanoparticles of different sizes. As the size of the gold nanoparticles increases, the localized surface plasmon resonance peak red-shifts. (C) Dark field images and corresponding spectra of different shapes of gold nanoparticles fabricated using electron-beam lithography. *(B) Reprinted with permission from reference Jana, N. R.; Gearheart, L.; Murphy, C. J. Seeding growth for size control of 5–40 Nm diameter gold nanoparticles. Langmuir 2001, 17 (22), 6782–6786. https://doi.org/10.1021/la0104323; Copyright (2001) American Chemical Society; (C) Reprinted with permission from reference Murray, W. A.; Barnes, W. L. Plasmonic materials. Adv. Mater. 2007, 19 (22), 3771–3782. https://doi.org/10.1002/adma.200700678.*

applications such as bio and chemical sensing, surface-enhanced phenomena such as SERS and surface-enhanced fluorescence. Another interesting aspect of LSP that differentiates them from SPPs is that LSP can be excited by direct illumination light without any special requirements. Thus, by shining light on a colloidal solution of gold nanoparticles yield interesting optical effects because of LSP excitation. The dependence of LSPR peaks on the refractive index of surrounding medium and strong local fields around plasmonic nanoparticles has been widely exploited in biological and chemical sensing applications [24–28].

As mentioned earlier, it is easy to excite surface plasmons on subwavelength noble metal nanoparticles. Unlike SPP excitations, LSP requires no special geometry such as total internal reflection or gratings. This is beneficial in applications wherein portability and cost-effectiveness is of significance. Moreover, it is easier to add multifunctionality to metal nanoparticles as will be seen in later sections. As this book brings out the relevance of multifunctional nanomaterials, we will focus on LSP of noble metal nanoparticles (gold/silver in particular) and its applications.

To understand LSP and its characteristics, simple classical scattering theories have been used as approximations. For example, for larger nanoparticles, i.e., particles have size greater than the wavelength of illuminating light, Mie's theory is utilized to explain the scattering and LSP excitations. Mie's scattering theory is based on finding an analytical solution to the Maxwell's equations and determining the scattered field when a uniform conducting sphere is illuminated with a plane electromagnetic wave [29]. The scattering fields obtained by solving the Maxwell equations are expanded in terms of vector harmonics. The theoretical approach is very rigorous and well-explained in several texts and references.

In a more interesting scenario of particle with size a comparable or smaller than the wavelength λ of the illumination light, Rayleigh scattering theory is often used. In this regime, it may be approximated that the phase of the oscillating electromagnetic field remains unchanged and a quasi-electrostatic approximation should suffice for solving the Maxwell's equations. When a spherical metal nanoparticle is exposed to light, the conduction electrons oscillate along with the external electromagnetic field in a coherent manner. The displacement in the electronic cloud creates an internal polarization and a restoring force that sets the oscillation going. The oscillation frequency is dependent on factors such as density of electrons, permittivity, size as well as shape of the nanoparticle. The frequency-dependent permittivity of the metal in Drude's approximation is given by [10].

$$\varepsilon(\omega) = 1 - \frac{ne^2}{\varepsilon_0 m\omega^2}, \tag{13.1}$$

where n is the number density of electrons, ε_0 is the electrical permittivity in vacuum, m is the mass of electrons, and ω is the frequency of light.

This expression is often written as

$$\varepsilon(\omega) = 1 - \frac{\omega_p^2}{\omega^2} \tag{13.2}$$

where $\omega_p^2 = \frac{ne^2}{\varepsilon_0 m}$ is termed the plasma frequency of the metal. In fact, if one considers the damping nature in bulk metals, an additional term including the damping factor γ needs to be added. The Eq. (13.2) then becomes

$$\varepsilon(\omega) = 1 - \frac{\omega_p^2}{\omega^2 + \gamma^2} \tag{13.3}$$

For noble metals in the visible and near-infrared frequencies, $\gamma \ll \omega$, and hence Eq. (13.2) is valid.

The polarizability induced in the metal nanoparticle by the oscillating electromagnetic field (light, for example) is given by the expression

$$\alpha(\omega) = 4\pi\varepsilon_0 a^3 \frac{\varepsilon(\omega) - \varepsilon_D(\omega)}{\varepsilon(\omega) + \varepsilon_D(\omega)} \tag{13.4}$$

where $\varepsilon_D(\omega)$ is the dielectric permittivity of the surrounding medium.

This has the form of the popular Clausius-Mossotti relation. An interesting outcome of this relation is that under the specific condition $Re[\varepsilon(\omega)] = -2\varepsilon_D$, the polarizability is a maximum. This means that the scattering cross section, which is related directly to the polarizability $\alpha(\omega)$ reaches a maximum often termed localized surface plasmon resonance (LSPR). For example, in the case of a colloidal solution of gold nanoparticles, the resonance wavelength is obtained at 520 nm, while for silver nanoparticles, the LSPR peaks in the blue to UV region. The size-dependent polarizability is useful for tuning and engineering the LSPR to the desired frequencies. The implication of this leads to the capability of metal nanoparticles as sensing platforms. This approximation is usually valid for small nanoparticles assuming to have a nearly spherical shape but may be extended to other shapes such as ellipsoids, cubes, and triangles.

The size and shape-tunable plasmonic resonance has a significant importance in biosensing applications where in it is desirable to have the LSPR closely matching the excitation wavelengths [28]. Owing to the recent advancements in nanofabrication tools and development in novel synthesis methods, it is now possible to achieve the desired size and shape of plasmonic nanoparticles. In particular, a whole gamut of shapes of noble nanoparticles has been synthesized using simple chemical reduction techniques. The most common ones include spheres, triangles [30,31], cubes [32–35], nanorods [36–38], nanostars [39–42], and nanoshells [43,44]. The bottom-up approach of chemical methods provides a facile route for the synthesis of the nanoparticles. In particular, gold and silver nanoparticles have been synthesized by the chemical reduction of chloride salts of the metal. For example, gold nanoparticles can be synthesized by the Turkevich method wherein chloroauric acid ($HAuCl_4$) in aqueous solution is reduced using reducing agents such as citric acid, ascorbic acid, sodium citrate, or trisodium citrate [45–47]. Gold nanorods have been synthesized using cetyltrimethylammonium bromide (CTAB) as the reducing agent [48,49]. CTAB also forms a capping agent for improving the stability of the nanoparticles in solution. Oleyamine and silver nitrate has been used to obtain gold and silver nanorods [50,51]. Large-sized gold nanoparticles can be synthesized using the seed-mediated method, where the growth takes place on small seed particles [23]. Gold nanostars have been synthesized using poly(vinylpyrrolidone) (PVP), N, N dimethylformamide (DMF), and silver nitrate for directional growth [39,40]. Gold nanoshells form an important class of plasmonic nanoparticles that possess interesting optical properties [44,52]. They were synthesized using a four-step process. First, silica cores are grown using Stöber method [53]. Next, the silica surface is functionalized with an amine containing compound aminopropyltriethoxysilane (APTES) [44]. This step facilitates the amine tails to stick out for adhesion of gold. The third step involves addition of gold precursor to the monodisperse colloidal solution of silica particles. The final step involves reduction of the gold salt to produce nanoparticles that attach to the amine tail on the silica. The gold particles form nucleation sites for further deposition and growth by Ostwald ripening. Further thickness of gold can be achieved by seed-mediated process.

Silver nanoparticles are usually synthesized using $AgNO_3$ precursor and a similar reduction process as that used for gold. Sodium borohydride, PVP, and DMF are commonly used as reducing agents [54,55].

Although chemical synthesis of plasmonic nanoparticles has been very popular owing to its simplicity and cost-effective nature, some applications require special designs or arrays of nanoparticles at specific distances. For such applications, a top-to-bottom approach of fabrication methods such as electron-beam lithography (E-beam lithography or EBL), focused-ion beam milling, or nanosphere lithography is more suitable. These fabrication tools, usually placed in clean-rooms, provide very structured and patterned distribution of nanoparticles. However, these methods require sophisticated, expensive instruments and are also time-consuming.

The most important property of plasmonic nanoparticles is the size and shape-dependent plasmonic resonances. This means that the LSPR of the plasmonic nanoparticles can be tuned from the ultraviolet, visible, and infrared frequencies simply by changing the size or shape of the nanoparticles. Plasmonic resonances are often observed by recording a UV-Vis-NIR absorption or scattering spectrum. The optical extinction of the nanoparticles is contributed by both absorption and scattering process, which in turn depends on the illumination light frequency. A typical extinction spectrum of a colloidal solution of gold nanoparticles synthesized using citrate reduction method is shown in Fig. 13.2B. As the size of the gold nanoparticle increases, the LSPR peaks red-shift. Dark field microscopy is one of the popular ways to observe the scattering from plasmonic nanoparticles as shown in Fig. 13.2C. One interesting way to tune the optical extinction of nanoparticles is by varying its aspect ratio (Fig. 13.3A). Changing the shape of the nanoparticles also affects

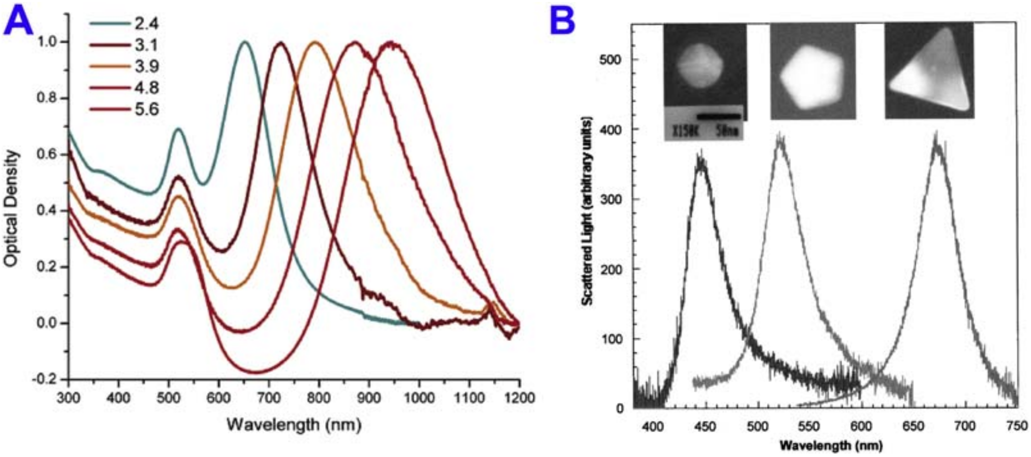

Figure 13.3

(A) Localized surface plasmon resonance (LSPR) spectra from UV-Vis absorption data for different aspect ratio of gold nanoparticle. As the aspect ratio is increased, the longitudinal LSPR (at the right) red-shifts, while the vertical peak remains constant. (B) LSPR spectra of different shapes of Ag nanoparticle. *(A) Reprinted with permission from reference Huang, X.; El-Sayed, I. H.; Qian, W.; El-Sayed, M. A. Cancer cell imaging and photothermal therapy in the near-infrared region by using gold nanorods. J. Am. Chem. Soc. 2006, 128 (6), 2115–2120. https://doi.org/10.1021/ja057254a; copyright (2006) American Chemical Society; (B) Reprinted with permission from reference Mock, J. J.; Barbic, M.; Smith, D. R.; Schultz, D. A.; Schultz, S. Shape effects in plasmon resonance of individual colloidal silver nanoparticles. J. Chem. Phys. 2002, 116 (15), 6755–6759. https://doi.org/10.1063/1.1462610.*

the optical properties in a significant way. For example, triangular gold nanoparticles have a red-shifted LSPR compared to spherical nanoparticles (Fig. 13.3C). For asymmetric nanoparticles, the polarization of incident light determines the spatial distribution local field. The tunable optical properties of noble metal nanoparticles make them excellent candidates for converting them as multifunctional nanoparticles.

3. Hybrid plasmonic nanomaterials

While plasmonic nanoparticles by themselves have interesting optical properties that has been exploited in several applications, researchers are now adding multifunctionality to the nanoparticles so as to increase their scope. Apart from the plasmonic properties, such hybrid plasmonic nanomaterials have other interesting features such as magnetic property, fluorescence, and refractory properties (Fig. 13.4). Such multifunctional hybrid plasmonic nanoparticles find application in biomedical diagnosis, sensing platforms as well as for the development of novel nanoscale devices. Consequently, there has been a growing number of research publications reporting multifunctional plasmonic nanoparticles and their applications. We will discuss some of the recent advances in the development of

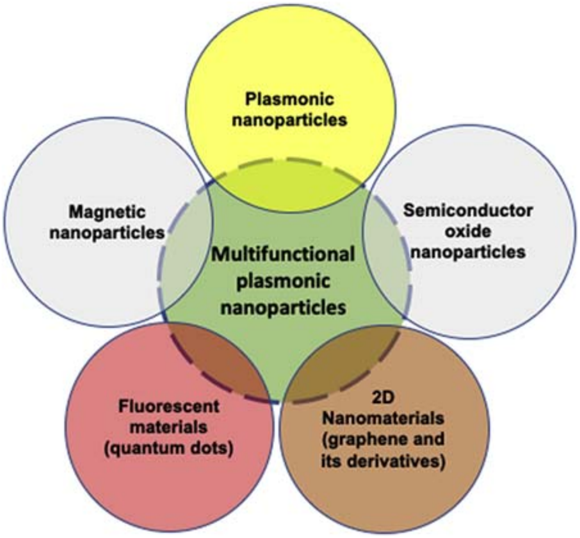

Figure 13.4

Plasmonic nanoparticles can be combined with other functional materials such as magnetic nanoparticles, quantum dots, wide band gap oxide nanoparticles, and two-dimensional materials such as graphene and its derivatives. The result of such combinations yields novel multifunctional nanomaterials that have interesting applications.

plasmonic-semiconductor core-shell systems, magnetic-plasmonic systems, fluorescent plasmonic nanoparticles, magnetic-fluorescent plasmonic nanoparticles, and graphene-gold nanocomposites.

4. Plasmonic-semiconductor core-shell nanoparticles

Wide band gap semiconductor oxide nanoparticles such as ZnO and TiO_2 have been studied extensively for their numerous physical and optical properties. These nanomaterials are found to be useful in catalysis, cosmetic and food industry, and biomedical applications. By combining with plasmonic metals, one can achieve an enhancement of the existing properties of these semiconductor nanoparticles or even achieve novel properties that are not observed in their native state. In this regard, plasmonic metal-semiconductor oxide core-shell nanoparticles or semiconductor-plasmonic core-satellite type nanoparticles have been synthesized and studied. Most popular among them are TiO_2 shell over Au, Pt, and Pd nanoparticles. TiO_2 nanoparticles are known for their photocatalytic activity and other light harvesting mechanisms. The inclusion of the plasmonic core enhances the photocatalytic capability of TiO_2 by increased absorption of light in the visible region, better electron trapping, and improving the electron-hole pair life time. One of the first reports in this direction was from Liz Marzan and co-workers where they reported the growth of TiO_2 layer on Ag nanoparticles [58]. The synthesis was done in a one-step process where in a silver precursor (silver nitrate) and a TiO_2 precursor was refluxed in a solvent mixture of ethanol and dimethylformamide. Another approach reported by Sakai et al. involves the growth of TiO_2 on Ag nanoparticles using a sol-gel method [59]. In a similar fashion, $Au-TiO_2$ core-shell nanostructures were also synthesized by Caruso and co-workers using polyelectrolyte linkers [60,61]. Zhang et al. synthesized plasmonic metal core-TiO_2 shell hybrid nanoparticles using a simple hydrothermal treatment of TiF_4 and noble metal nanoparticles (Au, Pt, and Pd) [62]. Improved photocatalytic stability was observed in these core-shell nanoparticles compared to bare TiO_2 nanoparticles. Several other configurations including Au decorated TiO_2, Au nano rod-TiO_2 core shell, and $SiO_2-Au-TiO_2$ hybrid nanostructures have also been reported for their improved photodegradation and photoelectrochemical water-splitting applications [63–66].

ZnO is another popular metal oxide semiconductor that has unique optical and physical properties that make them versatile material for several applications. High-chemical stability, strong absorption in the UV, photoluminescence in the UV-Vis wavelengths, and ease of synthesis make ZnO-plasmonic metal nanoparticles potential candidates for photocatalytic and light harvesting applications. Different geometries of combining plasmonic metal with ZnO has been reported of which core shell type nanoparticles have proven to be useful multifunctional nanoparticles in several studies [67,68]. The synthesis methods are similar to those used for plasmonic-TiO_2 nanoparticles. Recently, plasmon-ZnO hybrid nanoparticles have also been used in UV light detectors [69–74].

5. Magnetic-plasmonic nanoparticles

The combination of magnetic and plasmonic properties in the hybrid nanomaterials has potential applications in magnetic resonance imaging (MRI) as contrast agents, magnetic cell sorting applications, and cancer diagnosis as well as therapy [75–80]. Facile control over these nanoparticles using magnetic field allows for their transfer from one site to another, while the optical properties are being monitored. Iron oxide is one of the most common magnetic nanoparticles that has been used to synthesize these bifunctional nanomaterials. Very small nanoparticles of iron oxide are superparamagnetic and react only in the presence of an external magnetic field [81]. They are often used as therapeutic agents using hyperthermia in cancer patients. The two common configurations of core-shell magnetic-plasmonic nanomaterials are magnetic core-plasmonic shell and plasmonic core-magnetic shell. Gold nanoshells, having a dielectric material such as silica as the core material and a thin gold layer as shell, are an interesting class of plasmonic nanoparticles [44]. The optical properties of such gold nanoshells as their LSPR can be tuned from the visible to infrared by varying the core and shell diameters. Photothermal destruction of tumor cells, drug delivery, and SERS are some of the potential applications of these gold nanoshells [82,83]. Because of the special core-shell structure, gold nanoshells can have an interaction of the cavity and the sphere plasmon modes (Fig. 13.5A). This hybridization of the energy modes leads to an antisymmetric (antibonding) coupling with a higher energy and a symmetric (bonding) coupling with a lower energy (Fig. 13.5B) [85]. The strength of interaction is related to the aspect ratio of the shell and the core dielectric medium. On the other hand, iron oxides (Fe_3O_4 and Fe_2O_3) are the most popular magnetic nanoparticles that are used for synthesizing multifunctional nanoparticles. Fe_xO_y nanomaterials have a cubic inverse spinel structure that offers a good magnetic response to an external magnetic field [86,87].

Ultrasmall nanoparticles (usually less than 10 nm) with single magnetic domains behave as superparamagnetic materials making them useful in applications such as MRI contrast

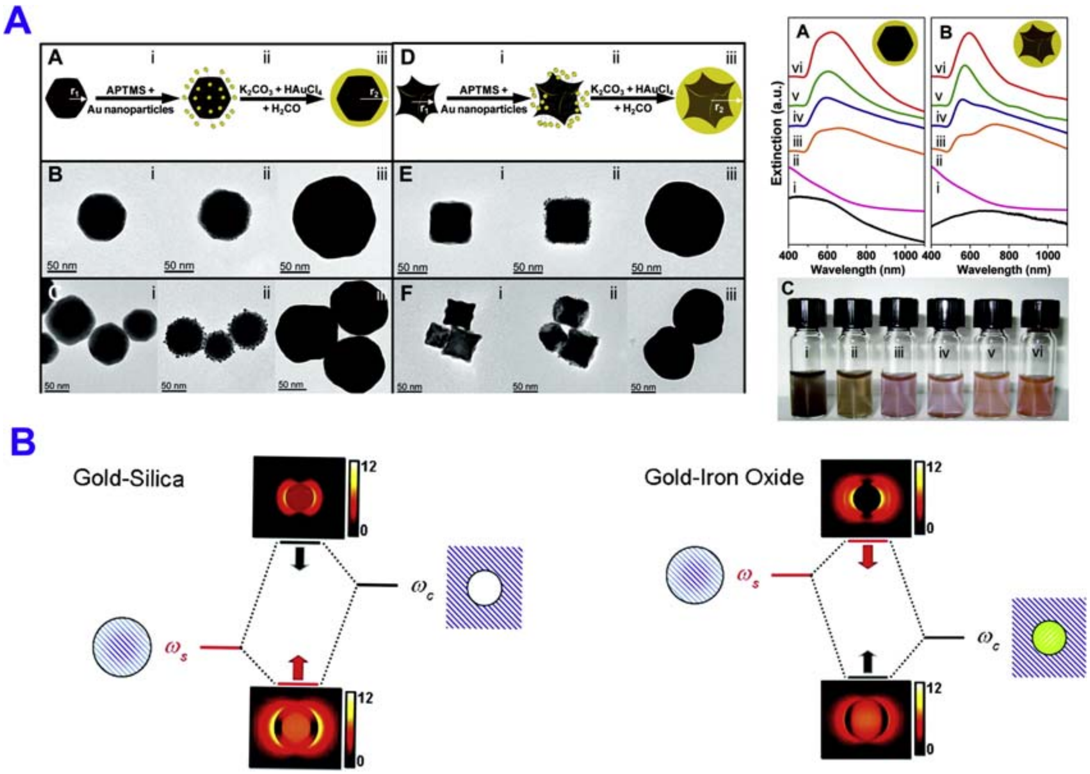

Figure 13.5

(A) Synthesis of different faceted gold-coated iron oxide nanoparticles. (B) Plasmon hybridization of core-shell nanoparticles based on the core material. Strong coupling leads to bonding or bright mode while poor coupling results in an antibonding or dark mode. *(B) Reprinted with permission from reference Levin, C. S.; Hofmann, C.; Ali, T. A.; Kelly, A. T.; Morosan, E.; Nordlander, P.; Whitmire, K. H.; Halas, N. J. Magnetic–plasmonic core–shell nanoparticles. ACS Nano 2009, 3 (6), 1379–1388. https://doi.org/10.1021/nn900118a; Copyright (2009) American Chemical Society.*

agents, cell separation, and magnetic field induced hyperthermia [88,89]. By combining the two functionalities, the nanoparticles have the potential for a wide spectrum of applications. The most common geometries that have been studied are Fe_3O_4 core and Au shell (Fe_3O_4@Au core-shell) and Fe_3O_4 core with Au satellites. Although there have been reports of study of the reverse combination of Au core- Fe_3O_4 shell (Au@ Fe_3O_4) [90,91], there has been more focus on magnetic material as core with plasmonic shell as the easily functionalizable plasmonic metal surface nanoparticle remains exposed.

Core-Satellite structures consist of a single magnetic core particle (usually below 200 nm in diameter) and small Au or Ag nanoparticles that are attached to the core [91–94]. The advantage of such core-satellite structures is that they form the intermediate step toward the formation of core-shell structures by seed-mediation. Moreover, as the satellite Au particles do not fully cover the magnetic core, there is possibility of utilizing the core surface for functionalization for certain applications. The large surface area of satellite plasmonic particles helps in applications such as catalysis and surface-enhanced phenomena.

The most popular core-satellite structure is Fe_3O_4@Au although other configurations have also been reported. The Fe_3O_4 core is usually synthesized using solvothermal or hydrothermal methods yielding nanoparticles of sizes less than 100 nm. Au nanoparticle satellites are then attached to the magnetic core nanoparticles using a chemical reduction of gold chloride salt [95,96]. One of the first such multifunctional nanoparticles consisted of a hybrid DNA functionalized magnetic-gold nanocomposite on silica particles [97]. Polymer links have also been employed to connect gold nanoparticles on the Fe_3O_4 magnetic core [98–100]. Here the polymer molecule not only protects the magnetic core from aggregation but also provides a way to attach plasmonic metals to the amine tails on the magnetic core. However, this technique is challenging as the surface of magnetic material is hydrophobic and requires further surface modification to attach the polymer.

Another configuration involves the addition of a silica spacer between the core and satellite particles. Using a sol-gel reaction process, it is possible to grow thin silica shells over the magnetic core nanoparticles [101]. The most common method to grow silica layers is by the Stöber process, where in tetraethylorthosilicate (TEOS) in an alcohol/water mixture is hydrolyzed followed by the deposition of silica. The thickness of the silica shell can be controlled by optimizing the concentration of TEOS. Further by functionalizing the silica by amine or thiol-containing ligands, it is possible to attach the gold seeds onto the silica surface. Another approach is to coat the magnetic core with a positively charged polymer (such as aniline) wherein the negatively charged Au nanoparticles can attach electrostatically. In another interesting method, small molecule amino acid (lysine) was attached to the magnetic core using its carboxylate end while its amine tail would stick out to facilitate the attachment of Au seeds. The distance between the magnetic core and the Au nanoparticles can be tuned by adjusting the length of the linker molecule.

The simplest way to synthesize magnetic core-Au shell composites is using a seed-mediated method. However, there are no easy ways to attach gold directly on to the Fe_3O_4 core structure. The magnetic material needs to be functionalized with amine-tailed compounds such as oleic acid-oleylamine or using a silica shell which can be easily functionalized with APTES. This is followed by a reduction of gold salt to form nanoparticle seeds that attach to the amine tails on the magnetic core structures. The core-satellite system of nanoparticles can be used for synthesizing core-shell nanostructures as the Au satellites act as nucleation and growth sites for Au atoms that are produced by further reduction of $HAuCl_4$. In fact, it is possible to synthesize different shapes as well as sizes of magnetic-core-Au shell type nanostructures using the seed-mediated method [102] (Fig. 13.6).

Apart from core-shell and core-satellite type magnetic-plasmonic nanoparticles, other geometries have also been shown to possess interesting magnetic and optical properties. Dumbbell-shaped Au—Fe_3O_4 nanoparticles, synthesized using the decomposition of iron pentacarbonyl ($Fe(CO)_5$) on Au nanoparticles and further oxidation to Fe_3O_4, were found to be efficient catalytic enhancers [110]. Hybrid colloidal structures involving the co-encapsulation of iron oxide and gold nanostars proved to be an effective way for SERS applications wherein the particles could be accumulated using an external magnet and then released back into solution [111]. In fact, Janus particles, whose surface contains two or more different physical and chemical properties, have shown to be promising candidates for several applications including biomedical science and nanotechnology. Magnetic plasmonic Janus nanoparticles consist of a magnetic nanoparticle attached to an Au nanoparticle.

For example, Janus magnetic nanostars with Au nanostars attached to an iron oxide nanosphere has been found to be useful as contrast agents for multimodal imaging [104,111,112]. The synthesis process involves the use of two seed-mediated methods: in the first step, gold seeds (nanospheres) are attached to iron oxide nanoparticles to form nanodumbbells, and in the second step, these nanodumbbells are used as seeds for asymmetric growth of nanostars. These nanoparticles show two distinct LSPR peaks in the visible range. The longer wavelength peak corresponds to the hybridization mode of the tip and body of the nanostar, while the shorter wavelength peak is the LSPR of the nanostar's body. The size of the Janus particles can be tuned by varying the ratio of the nanodumbell seeds to the gold salt during the synthesis process. These particles have shown to be useful as contrast agents in versatile imaging techniques including MRI, computed tomography, photoacoustic imaging, optical and SERS imaging.

Other forms of magnetic-plasmonic hybrid nanostructures have also been reported. For example, crystalline Fe—Au core-shell type nanostructures can be synthesized using physical deposition techniques [109]. Magnetic-plasmonic Au—Fe alloy nanoparticles have

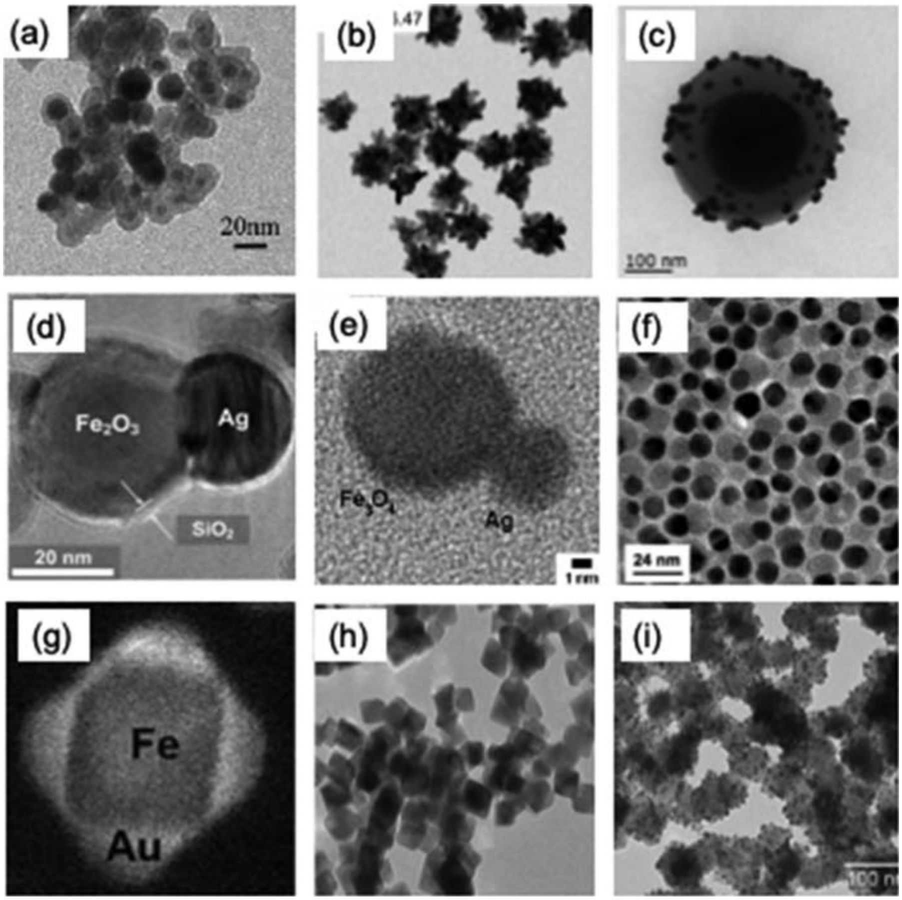

Figure 13.6

Representative TEM images of different types of magnetic-plasmonic nanoparticles. (A) Fe_3O_4 core-Au shell nanoparticles. (B) Star-like janus magnetic-Au nanoparticles. (C) Au satellites decorated Fe_3O_4@3-aminophenol-formaldehyde core-shell nanoparticles. (D) Silica-coated janus magnetic-plasmonic nanoparticles. (E) Heterodimer structure. (F) Dumbbell type bifunctional nanoparticle. (G) A crystalline Fe—Au core-shell nanoparticle. (H) and (I) Size and shape-controlled magnetic-Au nanoparticle. *(A) Reprinted with permission from reference Cho, S.-J.; Idrobo, J.-C.; Olamit, J.; Liu, K.; Browning, N. D.; Kauzlarich, S. M. Growth mechanisms and oxidation resistance of gold-coated iron nanoparticles. Chem. Mater. 2005, 17 (12), 3181—3186. https://doi.org/10.1021/cm0500713; Copyright (2005) American Chemical Society; (B) Reprinted with permission from referenceReguera, J.; Jiménez de Aberasturi, D.; Henriksen-Lacey, M.; Langer, J.; Espinosa, A.; Szczupak, B.; Wilhelm, C.; Liz-Marzán, L. M. Janus plasmonic—magnetic gold—iron oxide nanoparticles as contrast agents for multimodal imaging. nanoscale 2017, 9 (27), 9467—9480. https://doi.org/10.1039/C7NR01406F; (C) Reprinted with permission from reference Gong, C.; Li, Q.; Zhou, H.; Liu, R. Tiny Au satellites decorated Fe3O4@3-aminophenol-formaldehyde core-shell nanoparticles: easy synthesis and comparison in catalytic reduction for cationic and anionic dyes. Colloids Surfaces A Physicochem. Eng. Asp. 2018, 540, 67—72. https://doi.org/https://doi.org/10.1016/j.colsurfa.2017.12.045; (D) Reprinted with permission from reference Sotiriou, G. A.; Hirt, A. M.; Lozach, P.-Y.; Teleki, A.; Krumeich, F.; Pratsinis, S. E. Hybrid, silica-coated, janus-like plasmonic-magnetic nanoparticles. Chem. Mater. 2011, 23 (7), 1985—1992.*

also been synthesized using laser ablation of the alloy target in an ethanolic solution. These nanoparticles were successfully used as SERS substrates, MRI, and CT contrast agents [112]. In some reports, Ag nanoparticles have been used instead of Au as the shell plasmonic metal [113–115].

6. Applications of magnetic core-plasmonic shell nanoparticles

Owing to the multifunctional nature of magnetic-plasmonic hybrid nanoparticles, there are several avenues of applications for these nanomaterials that have been reported. One principal application for these multifunctional materials is in the biomedical imaging and cell separation [116,117]. Iron oxide nanoparticles have been used as T2 weighted contrast agents in MRI scanning, immunoassay studies, detoxification studies, hyperthermia, and for cell separation applications. However, MRI does not provide the resolution of optical images. The tunable plasmon excitation wavelength and easy functionalization of Au allows for easy biopenetration, selective targeting of cells or tissues for imaging and photothermal ablation. Furthermore, adding Au shell improves the biocompatibility of the nanoparticles. The plasmonic overcoating acts as a protective shell against corrosion of the magnetic nanoparticle in the biological solvents. Therefore, plasmonic shell-magnetic core nanoparticles have been recently used for targeted diagnosis and photothermal destruction of tumor cells. Gold-iron oxide core-shell nanoparticles were used as contrast agents for MRI scanning applications. For example, Sokolov et al. used core-shell γ -Fe_2O_3/Au nanoparticles for MRI imaging followed by photothermal destruction of cancer cells [118]. Halas and co-workers had used a gold shell over Fe_3O_4-doped silica core for enhancing both MRI as well as fluorescent images [119]. Human epidermal growth factor receptors

https://doi.org/10.1021/cm200399t; Copyright (2011) American Chemical Society; (E) Reprinted with permission from refernce Gu, H.; Yang, Z.; Gao, J.; Chang, C. K.; Xu, B. Heterodimers of nanoparticles: formation at a liquid–liquid interface and particle-specific surface modification by functional molecules. J. Am. Chem. Soc. 2005, 127 (1), 34–35. https://doi.org/10.1021/ja045220h; Copyright (2005) American Chemical Society; (F) Reprinted with permission from reference Yu, H.; Chen, M.; Rice, P. M.; Wang, S. X.; White, R. L.; Sun, S. Dumbbell-like bifunctional Au–Fe_3O_4 nanoparticles. Nano Lett. 2005, 5 (2), 379–382. https://doi.org/10.1021/nl047955q; Copyright (2005) American Chemical Society; (G) Reprinted with permission from reference Langlois, C.; Benzo, P.; Arenal, R.; Benoit, M.; Nicolai, J.; Combe, N.; Ponchet, A.; Casanove, M. J. Fully crystalline faceted Fe–Au core–shell nanoparticles. Nano Lett. 2015, 15 (8), 5075–5080. https://doi.org/10.1021/acs.nanolett.5b02273; Copyright (2015) American Chemical Society (H) and (I) Reprinted with permission from reference Kwizera, E. A.; Chaffin, E.; Shen, X.; Chen, J.; Zou, Q.; Wu, Z.; Gai, Z.; Bhana, S.; O'Connor, R.; Wang, L.; Adhikari, H.; Mishra, S. R.; Wang, Y.; Huang, X. Size- and shape-controlled synthesis and properties of magnetic–plasmonic core–shell nanoparticles. J. Phys. Chem. C 2016, 120 (19), 10530–10546. https://doi.org/10.1021/acs.jpcc.6b00875; Copyright (2016) American Chemical Society.

(HER2) are often used as targets for antibody therapy, especially in the case of breast cancers. Tumorous cells tend to overexpress this marker and can be used to detect early cancerous growths. By injecting the gold-Fe_3O_4 multifunctional nanocomposites conjugated with anti-HER2, it was possible to specifically attach the nanocomposites on the tumor cells. Using IR illumination, it was possible to destroy the tumor cells through photothermal cell death (Fig. 13.7A). In another report, Fan et al. demonstrated that aptamer-conjugated plasmonic/magnetic core-shell nanoparticles can be used for specific

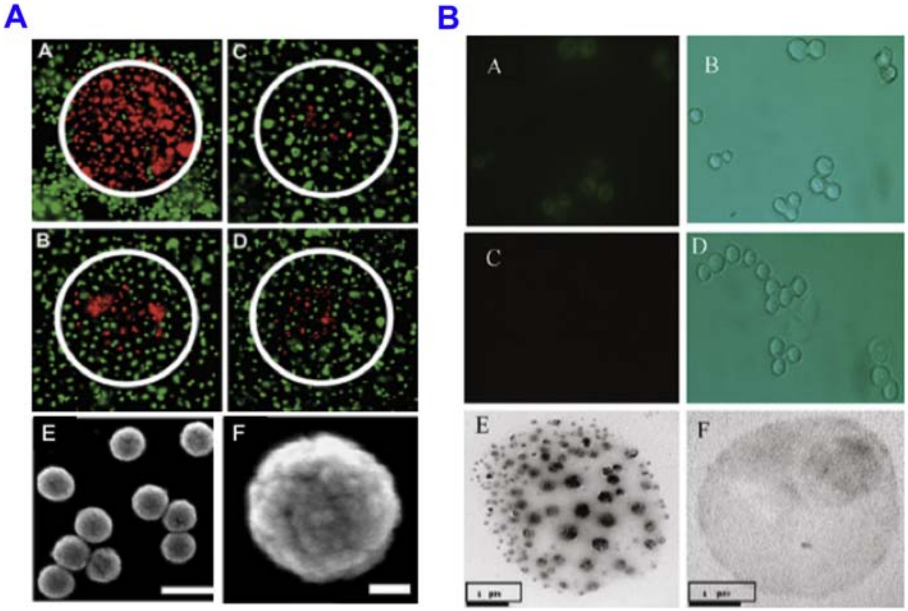

Figure 13.7

(A) Hyperthermia-induced cell death for SK-BR-3 (a) and MDA-MB-231 (c) cancer cells that have been incubated with the magnetic-plasmonic nanoparticles. (b) and (d) are images of the control experiments. NIR laser at 808 nm was used for photothermal cell death, (e) and (f) TEM images of the multifunctional nanoparticles. (B) Fluorescent images of a cancer cell (SK-BR-3) that has been attached with an aptamer conjugated magnetic-gold nanoparticles that has been separated magnetically from a mixture of LNCaP and SK-BR-3 cancer cells (b) Bright field image of the same (c) Fluorescence image of LNCaP. Note that SK-BR3 cannot be seen here. (d) Bright field image of the same (e) TEM image of SK-BK-3 cell which shows the attached magnetic-plasmonic nanoparticles. (f) TEM image of LNCaP cell. *(A) Taken from reference Bardhan, R.; Chen, W.; Perez-Torres, C.; Bartels, M.; Huschka, R. M.; Zhao, L. L.; Morosan, E.; Pautler, R. G.; Joshi, A.; Halas, N. J. Nanoshells with targeted simultaneous enhancement of magnetic and optical imaging and photothermal therapeutic response. Adv. Funct. Mater. 2009, 19 (24), 3901–3909. https://doi.org/10.1002/adfm.200901235; (B) Reprinted with permission from reference Fan, Z.; Shelton, M.; Singh, A. K.; Senapati, D.; Khan, S. A.; Ray, P. C. Multifunctional plasmonic shell–magnetic core nanoparticles for targeted diagnostics, isolation, and photothermal destruction of tumor Cells. ACS Nano 2012, 6 (2), 1065–1073. https://doi.org/10.1021/nn2045246; Copyright (2012) American Chemical Society.*

binding, imaging, and magnetic separation of four different cancer cells [120]. These cancer cell lines include the human breast cancer cell lines SK-BR-3, HER2-negative human breast cancer MDA-MB cell line, the human prostate cancer cell line LNCaP, and human skin cancer HaCaT cell line. The magnetic-plasmonic core-shell nanoparticles are attached with Cy3-modified S6 aptamers using the −SH ligand. Magnetic cell separation and fluorescence imaging was possible after binding the multifunctional nanoparticle onto the cancer cells (Fig. 13.7B). Hyperthermia was introduced using a 670 nm laser at 2−3 W/cm^2 of intensity for the cancer cell destruction. There has been a plethora of reports on using magnetic-plasmonic multifunctional nanoparticles for imaging and photothermal destruction of tumor cells. There are several review papers on this specific application of multifunctional magnetic-plasmonic nanoparticles that the readers may find interesting [121−124].

Magnetic-plasmonic nanoparticles also find applications in enhanced-spectroscopic measurements such as SERS [125,126]. The main advantage of using a magnetic core is that it allows for better control of the electromagnetic hot-spot formation in the liquid medium using an external magnetic field. The hybrid nanoparticles can be easily aggregated at the required site using an external magnet and then released back into the medium after Raman measurements. This has been exploited in sensing and detecting several analytes including thiols, biochemicals such as amino acids, drugs, pesticides, and chemical pollutants. In this regard, Ag nanoparticles on the magnetic core are more advantageous as they show better SERS capability compared to Au. An overview of different modalities of multifunctional gold-magnetic nanocomposites can be obtained from the review article by Leung et al. [127].

7. Fluorescent-plasmonic nanoparticles

The combination of fluorescence with plasmonic properties can be beneficial in direct imaging applications. It also leads to the observation of interesting physical phenomena such as metal-enhanced fluorescence and quenching. Although plasmonic nanoparticles by themselves have no significant photoluminescence, clusters of Au or Ag have shown to emit light under excitation [128−131]. For application point of view, it is more interesting to attach a strong fluorescent emitter such as quantum dots to plasmonic metals. Quantum dots are robust emitters that can withstand photobleaching, and their emission can be tuned by varying the size. The effect of placing emitters in the vicinity of plasmonic metals has been of great interest as the plasmonic fields can alter the emission properties in a significant way. For example, it is reported that when CdSe/ZnS core-shell quantum dots were placed on gold nanoparticles with a polyelectrolyte spacer, the luminescence of the quantum dots is enhanced by a factor of five for a spacer thickness of 11 nm [132]. In absence of the spacer layer, the luminescence is reduced by a factor of three because of quenching process. In fact, it is also possible to excite surface plasmons in metal when a fluorophore is placed in close vicinity. This phenomenon, called as surface plasmon coupled emission or SPCE, has been exploited in optoelectronic and sensing devices. SPPs on thin metal films can also be harnessed to enhance fluorescence emission although it requires special coupling geometry.

There has been a plethora of reports on the interaction between fluorophore molecules and plasmonic metals [133]. The distance-dependent interaction can lead to either an enhancement of the fluorescence or a quenching in fluorescence when the molecule is very close to the metal surface.

A more interesting configuration for application point of view is the development of hybrid quantum dot-plasmonic nanoparticles. Quantum dots are ultrasmall (usually less than 10 nm) semiconductor or metal nanoparticles that show a size-dependent emission property. Quantum dots usually have broad excitation spectrum that allows their applications in different light sources. They also have a very narrow emission bandwidth which can be exploited in multicolor imaging schemes. The strong confinement of electrons in these sub-10 nm nanocrystals leads to size-tunable band gaps and emission. Other advantageous including reduced photobleaching, longer stability, and shelf life, and very high quantum yield makes them potential materials as replacement for organic dye molecules. However, there are two major disadvantages of using quantum dots for imaging applications. First one is regarding the degradation of the material composition under prolonged excitation of the quantum dots. Secondly, the emission fluctuation, also called blinking, of the single quantum dots can be an issue in very low-light experiments. While the former is intrinsic to the quantum dots, the later arises because of nonradiative recombination (also called Auger recombination). Nevertheless, these problems can be resolved to certain extent by using plasmonic shells or attaching the quantum dots to plasmonic metals. Direct contact of quantum dots with plasmonic metals can lead to fluorescence quenching through charge-transfer mechanisms. Hence a spacer dielectric or a polymer molecule is sandwiched between the two resulting in a hybrid multifunctional nanoparticle system. The distance between the quantum dot and the plasmonic metal can be tuned by varying the thickness of the dielectric material (usually silica) or by changing the length of the linker molecule.

Two different geometries of quantum dot-plasmonic metal hybrid nanoparticles have been reported so far. The first one is a core-shell type structure, wherein the quantum dot is covered with a shell of plasmonic metal with a thin spacer in between [134,135]. Gold-encapsulated quantum dots have certain advantages including improved efficiency, improved stability, easy functionalization on the gold shell, and reduced toxicity of the quantum dots (which usually contains toxic metals such as Cd or Pb). However, it should be noted that a very thick shell of gold can deteriorate the emission transmission while too thin shells can lead to unwanted scattering or exposed quantum dot surfaces. Hence a precise control of the deposition process is necessary to obtain ideal configuration of gold-shell quantum dots. The synthesis method is often a two-step or three-step process. In one method reported by Jin and Gao, single quantum dots are coated with a layer of peptide, poly-L-histidine (PLH) that acts as a linker molecule to the outer gold shell (Fig. 13.8) [134]. The strong affinity of gold toward histidine molecules has been exploited in this work to grow gold on the quantum dots. In the synthesis process, quantum dots are first functionalized with trioctylphosphine oxide and then coated with PLH. $HAuCl_4$ is then reduced using hydroxylamine to obtain Au^{3+} ions that attach on the histidine molecules. The distance between the quantum dot and the gold ions were adjusted using additional

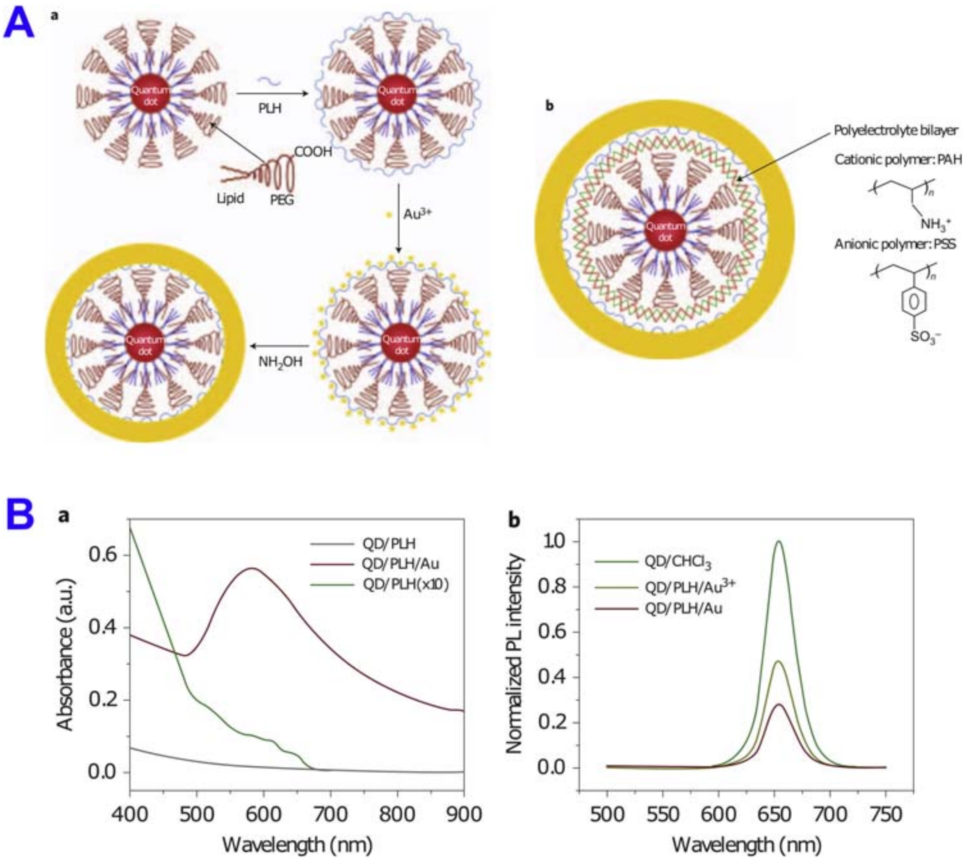

Figure 13.8

Plasmonic fluorescent quantum dots (A) Synthesis method for coating Au over the quantum dot using a polymer linker (B) Absorption spectrum of the quantum dot before and after coating with Au. The plasmonic LSPR of gold shell can be observed (C) emission spectra of the quantum dot before and after Au coating. *(C) Reprinted with permission from reference Jin, Y.; Gao, X. Plasmonic fluorescent quantum dots. Nat. Nanotechnol. 2009, 4 (9), 571–576.* https://doi.org/10.1038/nnano.2009.193.

polyelectrolyte bilayers using a layer-by-layer assembly process. This synthesis technique yielded in core-shell quantum dots with a 3−5 nm gold shell at a distance of >3 nm from the core. Optical absorption measurements on the gold encapsulated core-shells revealed the suppression of quantum dot absorption peaks by the gold shell LSPR. From the fluorescence measurements, it was observed that the quantum yield of the lipid-coated quantum dots remained similar to the bare quantum dots while that for the gold-encapsulated quantum dots reduced to 18%. However, no shift in the emission peaks was seen in the gold-encapsulated quantum dots. It was also reported that the thickness of gold shell played a significant role in the emission intensity. Gold layers thicker than 5 nm significantly diminished the transmission of the fluorescence emitted by the quantum dots.

In a different approach, Botao Ji et al. first encapsulated the quantum dots with a thin layer of silica and then attached gold shell to the silica layer [135]. This was achieved in a three-step process. First, the quantum dot was encapsulated in a thin silica layer using the hydrolysis of TEOS by water-in-oil microemulsion process (Fig. 13.9A). Next, a polymer molecule, poly(1-vinylimidazole co-vinyltrimethoxysilane) (PVIS) was attached onto the silica surface. This polymer ensured the maximization of adsorption of gold seeds. Finally, gold ions were added and reduced using formaldehyde to get a continuous shell of gold around the silica coated quantum dots. The gold shell not only improved the robustness of the quantum dots but also provided a local enhanced field for better emission properties. From the time-resolved fluorescence measurements on the golden quantum dots, it was observed that the life-time of emission was reduced to 20 ns from 160 ns of bare quantum dots. This decrease in fluorescence life time was attributed to the strong coupling of the gold shell plasmons with the quantum dote core. It was also observed that there was no fluctuation of emission, and the photoluminescence spectrum showed a Poissonian intensity distribution. This means that the quantum dots were nonblinking unlike bare ones (Fig. 13.9B). Such nonblinking property of gold encapsulated quantum dots was attributed to the suppression of nonradiative Auger process thereby allowing the quantum dots to exhibit multiexciton emission. These multifunctional quantum dots are potential candidates for multicolor bioimaging as well as in optoelectronic applications.

Another interesting configuration is to attach quantum dots on gold nanoparticles like satellites [136]. Such a geometry facilitates the study of exciton-plasmon interaction and metal-enhanced fluorescence phenomenon. In this regard, there have been different approaches to attach quantum dots on the gold nanoparticles. For example, DNA-based self-assembly process can form quantum dot-plasmonic nanoparticle hybrid system with good control. Cohen-Hoshen et al. used such a self-assembly method to attach quantum dots to gold nanoparticles [137]. For this, gold nanoparticles, prepared by citrate reduction of gold salt, were used as seed to grow larger gold nanoparticles of 80 nm size. These

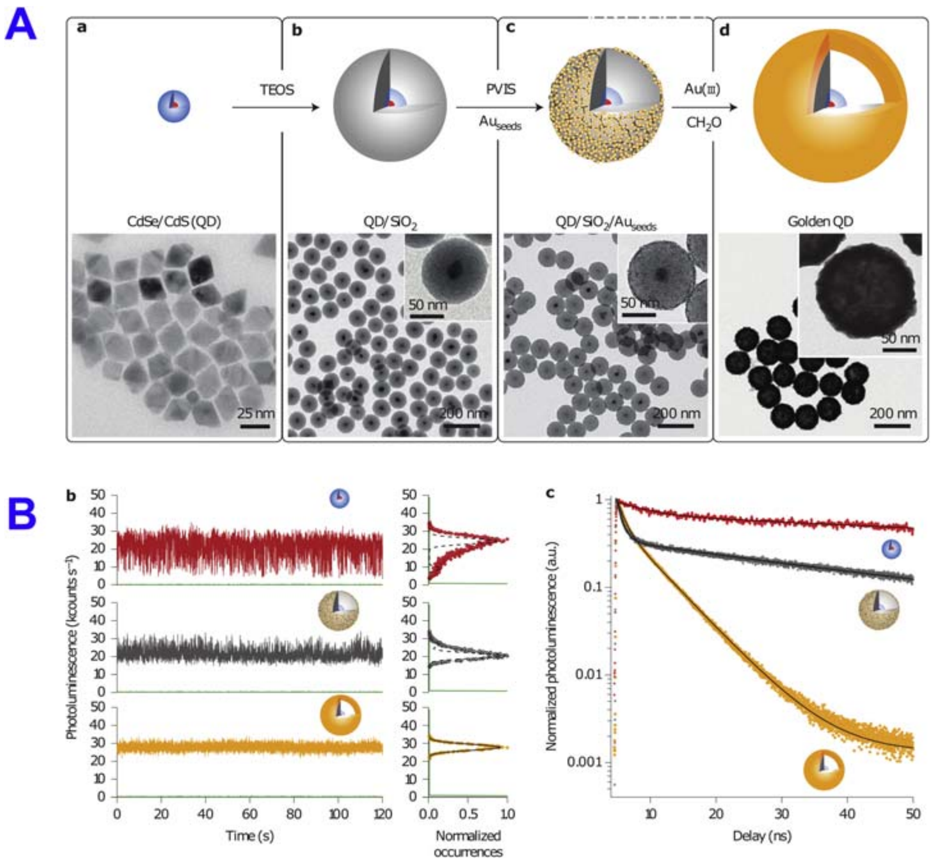

Figure 13.9

Gold-encapsulated core-shell quantum dots (A) Synthesis scheme for encapsulating quantum dots in gold. Here a thin silica layer is used as spacer. TEM images at each step are also shown. (B) Suppression of blinking behavior of quantum dots after encapsulation with gold. (C) Evolution of decay of fluorescence of the quantum dots before and after coating of gold. *(C) Reprinted with permission from reference Ji, B.; Giovanelli, E.; Habert, B.; Spinicelli, P.; Nasilowski, M.; Xu, X.; Lequeux, N.; Hugonin, J.-P.; Marquier, F.; Greffet, J.-J.; Dubertret, B. Non-blinking quantum dot with a plasmonic nanoshell resonator. Nat. Nanotechnol. 2015, 10 (2), 170–175. https://doi.org/10.1038/nnano.2014.298.*

nanoparticles were then functionalized with a thiol-DNA-biotin molecule. The thiol end attaches to the gold surface, while the biotin is used to link the CdSe/ZnS core shell type quantum dots coated with streptavidin. A strong polarization-dependent emission was observed in the hybrid system. Such hybrid systems constitute interesting platform for studying the interaction of single emitters with plasmonic metal nanoparticles. They also find applications in multipurpose functionalities such as bioimaging and photothermal treatment of tumorous cells.

8. Fluorescent-magnetic-plasmonic nanoparticles

In spite of the recent advances in nanoparticle synthesis and nanofabrication methods, combining of the three functional properties: fluorescence, magnetic, and plasmonic properties in a single nanostructure is still considered to be a big challenge. As the merging of different properties may lead to undesirable effects, it is necessary to study the interaction of individual properties with each other and then develop a protocol for the synthesis. For example, fluorescence can get quenched if the quantum dot is in direct contact with the plasmonic metal while adding spacer layers can hinder magnetic properties. However, there has been some effort in this direction to develop such multifunctional nanomaterials owing to their potential applications.

9. Graphene-plasmonic nanocomposites

In the recent years, graphene and its derivatives (for example, graphene oxide reduced graphene oxide) have been researched intensively for their interesting physical, optical, and electronic properties [138]. It has been known that the sp^2 hybridization in graphene-like structures facilitate the functionalization of several types of molecules and for the study of aromatic molecular interaction from the π-π type layers. Owing to the electronic properties of graphene, it has been seen as a potential SERS substrate yielding large chemical enhancements [139,140]. In fact, it has been reported that mildly reduced graphene, rather than pristine graphene, offers better chemical enhancement in SERS [141]. By combining plasmonic metal nanostructures with graphene, it is possible to attain large enhancement in Raman scattering from molecules [142,143]. While the graphene support offers chemical enhancement, the intense local fields of surface plasmons in plasmonic nanoparticles gives rise to large electromagnetic enhancements. Thus, the underlying graphene layer not only provides the necessary support for the plasmonic metal but also participates in the SERS mechanism. In this regard, graphene oxide is a better choice than graphene as the dangling bonds of different hydroxyl and carboxyl groups forms sites for functionalization. The two ways of integrating graphene type materials with plasmonic metal nanoparticles are shown in Fig. 13.10A. The graphene sheet can be conjugated with gold or silver nanoparticles or the nanoparticles can be wrapped with graphene layers. Using a one-pot synthesis method, Hu et al. fabricated reduced graphene oxide and silver nanoparticle hybrids as Raman reporters for the detection of folic acid as potential application toward cancer diagnostics [147]. Nergiz et al. reported the synthesis of gold nanorod-graphene oxide nanorolls using a self-assembly method [148]. Liz Marzan's group used a two-step method to synthesize reduced graphene oxide-gold nanostar hybrid nanocomposite for SERS applications (Fig. 13.10B) [145]. Another interesting method reported by Nair et al. involves the synthesis of different plasmonic nanostructures such as silver nanospheres, nanocubes, and nanowires over Boron-doped graphene sheets using an in-situ method [149]. For SERS and photocatalytic applications,

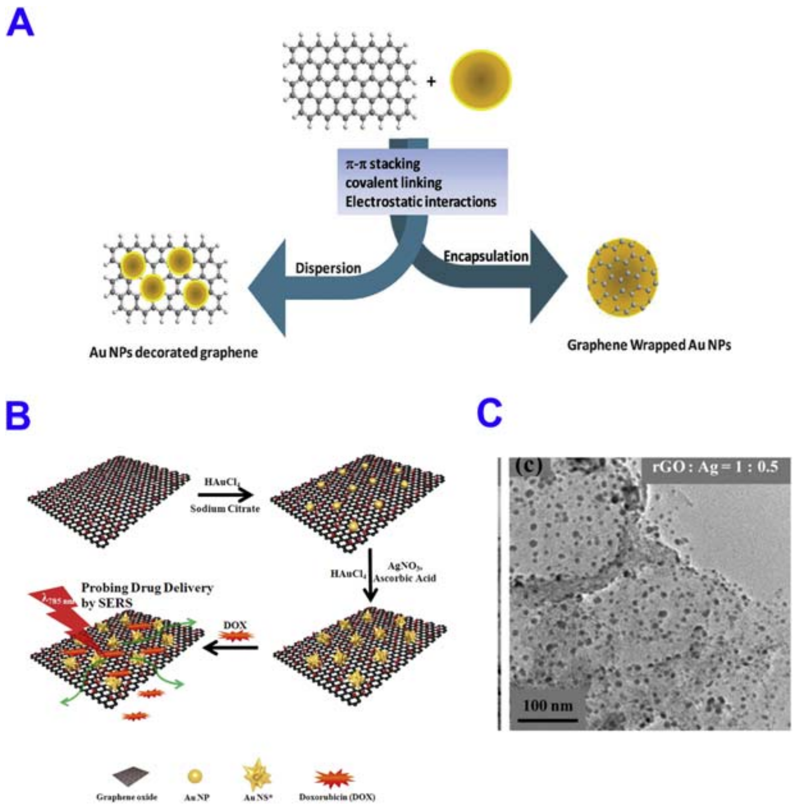

Figure 13.10

(A) Different modalities used for graphene oxide-plasmonic nanoparticle composites (B) Synthesis scheme for reduced graphene oxide-gold nanostar composite for SERS applications. (C) SEM image of reduced graphene oxide-silver nanoparticles. *(A) Reprinted with permission from reference Turcheniuk, K.; Boukherroub, R.; Szunerits, S. Gold–graphene nanocomposites for sensing and biomedical applications. J. Mater. Chem. B 2015, 3 (21), 4301–4324. https://doi.org/10.1039/C5TB00511F; (B) Reprinted with permission from reference Wang, Y.; Polavarapu, L.; Liz-Marzán, L. M. Reduced graphene oxide-supported gold nanostars for improved SERS sensing and drug delivery. ACS Appl. Mater. Interfaces 2014, 6 (24), 21798–21805. https://doi.org/10.1021/am501382y; Copyright (2014) American Chemical Society; (C) Reprinted with permission from reference Bhunia, S. K.; Jana, N. R. Reduced graphene oxide-silver nanoparticle composite as visible light photocatalyst for degradation of colorless endocrine disruptors. ACS Appl. Mater. Interfaces 2014, 6 (22), 20085–20092. https://doi.org/10.1021/am505677x; Copyright (2014) American Chemical Society.*

silver is considered superior to gold. In this regard, Ag nanoparticle decorated reduced graphene sheets have also been synthesized [146]. The hybrid structures were used as SERS platform for enzyme-free detection of hydrogen peroxide. In a recent work, a hybrid structure based on graphene oxide with plasmonic and magnetic nanostructures were used for selective separation and label-free identification of Alzheimer's disease biomarkers.

A review of the different configurations of graphene and plasmonic metal nanocomposites can be found in Ref. [144]. Graphene and its derivates have also been known to have good photothermal properties that can be exploited in applications such as optical trapping and assembly of nanoparticles [157], and photothermal ablation of biological samples such as bacteria [153]. In conjuction with plasmonic nanoparticles, it is possible to enhance the ohotothermal properties of graphene and further the scope of their applications. Graphene oxide-plasmonic nanoparticle composites are promising SERS substrates for numerous applications including biodetection, chemical pollutant detection, and optoelectronic nanoscale devices [150–156].

10. Future prospects of multifunctional plasmonic nanomaterials

Adding multifunctionality to existing properties of plasmonic nanoparticles is always advantageous for diversifying their applications. A lot of effort has been put in this direction, especially for their biomedical imaging and detection capabilities. One important application for such multifunctional plasmonic nanoparticles is for the early detection and treatment of cancers. In the recent years, there has been an exponential rise in the number of cancer patients worldwide. Owing to this increase, researchers are turning toward nanotechnology-based solutions for early cancer detection and treatment. In this regard, multifunctional nanomaterials have been considered as potential imaging markers as well as photothermal agents. In particular, multifunctional plasmonic nanoparticles have been reported to be useful in identifying the cancer cells and selectively destroy the tumorous tissues using photothermal methods. Plasmonic nanoparticles and superparamagnetic nanoparticles by themselves have been found as potential nanomaterials for such biomedical applications and therapeutics. Because of their unique properties, plasmonic nanoparticles (gold, in particular) have been researched for their bioimaging and photothermal therapeutic agents. On the other hand, iron oxide–based nanoparticles have been employed in MRI scanning as contrast agents and hyperthermia for tumor cell destruction. By combining these two functional nanoparticles, it is possible to diversify their capabilities as a detection and treatment mechanism for common cancers.

There are several challenges that need to be overcome before clinical trials of these multifunctional nanoparticles are carried out in real patients. It is important that the nanoprobes used have high specificity toward the tumor cells and minimal bioaccumulation. The ease of availability and cost of synthesis also need to be taken into consideration. On the above, the side effects of nanoparticles in human system are still not fully understood. It is however clear that owing to their multitasking capabilities such functional plasmonic nanomaterials offer great possibility for biomedical applications in the near-future.

References

[1] R. Zsigmondy, Ueber Wässrige Lösungen Metallischen Goldes, Justus Liebigs Ann. Chem. 301 (1) (1898) 29–54, https://doi.org/10.1002/jlac.18983010104.

[2] R.W. Wood, On a remarkable case of uneven distribution of light in a diffraction grating spectrum, Proc. Phys. Soc. London 18 (1) (1902) 269–275, https://doi.org/10.1088/1478-7814/18/1/325.

[3] J.W. Strutt, On the dynamical theory of gratings, Proc. R. Soc. Lond. - Ser. A Contain. Pap. a Math. Phys. Charac. 79 (532) (1907) 399–416, https://doi.org/10.1098/rspa.1907.0051.

[4] U. Fano, The theory of anomalous diffraction gratings and of quasi-stationary waves on metallic surfaces (sommerfeld's waves), J. Opt. Soc. Am. 31 (3) (1941) 213–222, https://doi.org/10.1364/JOSA.31.000213.

[5] R.H. Ritchie, Plasma losses by fast electrons in thin films, Phys. Rev. 106 (5) (1957) 874–881, https://doi.org/10.1103/PhysRev.106.874.

[6] C.J. Powell, J.B. Swan, Origin of the characteristic electron energy losses in aluminum, Phys. Rev. 115 (4) (1959) 869–875, https://doi.org/10.1103/PhysRev.115.869.

[7] E.A. Stern, R.A. Ferrell, Surface plasma oscillations of a degenerate electron gas, Phys. Rev. 120 (1) (1960) 130–136, https://doi.org/10.1103/PhysRev.120.130.

[8] H.A. Atwater, The Promise of Plasmonics, Scientific American, 2007.

[9] W.A. Murray, W.L. Barnes, Plasmonic materials, Adv. Mater. 19 (22) (2007) 3771–3782, https://doi.org/10.1002/adma.200700678.

[10] S.A. Maier, Plasmonics: Fundamentals and Applications, Springer, New York, 2007, https://doi.org/10.1007/0-387-37825-1.

[11] W.L. Barnes, A. Dereux, T.W. Ebbesen, Surface plasmon subwavelength optics, Nature 424 (6950) (2003) 824–830, https://doi.org/10.1038/nature01937.

[12] T.J. Davis, D.E. Gómez, A. Roberts, Plasmonic circuits for manipulating optical information, Nanophotonics 6 (3) (2016) 543–559, https://doi.org/https://doi.org/10.1515/nanoph-2016-0131.

[13] J. Homola, S.S. Yee, G. Gauglitz, Surface plasmon resonance sensors: review, Sensor. Actuator. B Chem. 54 (1) (1999) 3–15, https://doi.org/10.1016/S0925-4005(98)00321-9.

[14] J. Homola (Ed.), Surface Plasmon Resonance Based Sensors, Springer, Berlin, Heidelberg, 2006, https://doi.org/10.1007/b100321.

[15] I. Abdulhalim, M. Zourob, A. Lakhtakia, Surface plasmon resonance for biosensing: a mini-review, Electromagnetics 28 (3) (2008) 214–242, https://doi.org/10.1080/02726340801921650.

[16] J. Homola, Surface plasmon resonance sensors for detection of chemical and biological species, Chem. Rev. 108 (2) (2008) 462–493, https://doi.org/10.1021/cr068107d.

[17] J. Homola, Surface plasmon resonance biosensing, in: CLEO/Europe - EQEC 2009 - European Conference on Lasers and Electro-Optics and the European Quantum Electronics Conference, 2009, p. 1, https://doi.org/10.1109/CLEOE-EQEC.2009.5196286.

[18] H. Raether, Surface Plasmons on Smooth and Rough Surfaces and on Gratings, Springer, 1988.

[19] J.M. Pitarke, V.M. Silkin, E.V. Chulkov, P.M. Echenique, Theory of surface plasmons and surface-plasmon polaritons, Rep. Prog. Phys. 70 (1) (2006) 1–87, https://doi.org/10.1088/0034-4885/70/1/r01.

[20] A.V. Zayats, I.I. Smolyaninov, A.A. Maradudin, Nano-optics of surface plasmon polaritons, Phys. Rep. 408 (3) (2005) 131–314, https://doi.org/10.1016/j.physrep.2004.11.001.

[21] J.-J. Greffet, in: S. Enoch, N. Bonod (Eds.), Introduction to Surface Plasmon Theory BT - Plasmonics: From Basics to Advanced Topics, Springer Berlin Heidelberg, Berlin, Heidelberg, 2012, pp. 105–148, https://doi.org/10.1007/978-3-642-28079-5_4.

[22] V.G. Achanta, Surface waves at metal-dielectric interfaces: material science perspective, Rev. Phys. 5 (2020) 100041, https://doi.org/10.1016/j.revip.2020.100041.

[23] N.R. Jana, L. Gearheart, C.J. Murphy, Seeding growth for size control of 5–40 Nm niameter gold nanoparticles, Langmuir 17 (22) (2001) 6782–6786, https://doi.org/10.1021/la0104323.

[24] J. Zhao, X. Zhang, C.R. Yonzon, A.J. Haes, R.P. Van Duyne, Localized surface plasmon resonance biosensors, Nanomedicine 1 (2) (2006) 219−228, https://doi.org/10.2217/17435889.1.2.219.
[25] K.A. Willets, R.P. Van Duyne, Localized surface plasmon resonance spectroscopy and sensing, Annu. Rev. Phys. Chem. 58 (1) (2007) 267−297, https://doi.org/10.1146/annurev.physchem.58.032806.104607.
[26] S. Unser, I. Bruzas, J. He, L. Sagle, Localized surface plasmon resonance biosensing: current challenges and approaches, Sensors 15 (7) (2015) 15684−15716, https://doi.org/10.3390/s150715684.
[27] P. Singh, in: C.D. Geddes (Ed.), LSPR Biosensing: Recent Advances and Approaches BT - Reviews in Plasmonics 2016, Springer International Publishing, Cham, 2017, pp. 211−238, https://doi.org/10.1007/978-3-319-48081-7_10.
[28] K.M. Mayer, J.H. Hafner, Localized surface plasmon resonance sensors, Chem. Rev. 111 (6) (2011) 3828−3857, https://doi.org/10.1021/cr100313v.
[29] C.F.B.D.R. Huffman, Absorption and Scattering of Light by Small Particles, WILEY-VCH Verlag GmbH & Co. KGaA, 1998.
[30] C. Kuttner, M. Mayer, M. Dulle, A. Moscoso, J.M. López-Romero, S. Förster, A. Fery, J. Pérez-Juste, R. Contreras-Cáceres, Seeded growth synthesis of gold nanotriangles: size control, SAXS analysis, and SERS performance, ACS Appl. Mater. Interface. 10 (13) (2018) 11152−11163, https://doi.org/10.1021/acsami.7b19081.
[31] L. Scarabelli, M. Coronado-Puchau, J.J. Giner-Casares, J. Langer, L.M. Liz-Marzán, Monodisperse gold nanotriangles: size control, large-scale self-assembly, and performance in surface-enhanced raman scattering, ACS Nano 8 (6) (2014) 5833−5842, https://doi.org/10.1021/nn500727w.
[32] M. Haggui, M. Dridi, J. Plain, S. Marguet, H. Perez, G.C. Schatz, G.P. Wiederrecht, S.K. Gray, R. Bachelot, Spatial confinement of electromagnetic hot and cold spots in gold nanocubes, ACS Nano 6 (2) (2012) 1299−1307, https://doi.org/10.1021/nn2040389.
[33] Q.-Y. Lin, Z. Li, K.A. Brown, M.N. O'Brien, M.B. Ross, Y. Zhou, S. Butun, P.-C. Chen, G.C. Schatz, V.P. Dravid, K. Aydin, C.A. Mirkin, Strong coupling between plasmonic gap modes and photonic lattice modes in DNA-assembled gold nanocube arrays, Nano Lett. 15 (7) (2015) 4699−4703, https://doi.org/10.1021/acs.nanolett.5b01548.
[34] D. Lee, S. Yoon, Gold nanocube−nanosphere dimers: preparation, plasmon coupling, and surface-enhanced raman scattering, J. Phys. Chem. C 119 (14) (2015) 7873−7882, https://doi.org/10.1021/acs.jpcc.5b00314.
[35] C. Deeb, X. Zhou, R. Miller, S.K. Gray, S. Marguet, J. Plain, G.P. Wiederrecht, R. Bachelot, Mapping the electromagnetic near-field enhancements of gold nanocubes, J. Phys. Chem. C 116 (46) (2012) 24734−24740, https://doi.org/10.1021/jp304647e.
[36] A. Gole, C.J. Murphy, Seed-mediated synthesis of gold nanorods: role of the size and nature of the seed, Chem. Mater. 16 (19) (2004) 3633−3640, https://doi.org/10.1021/cm0492336.
[37] J. Pérez-Juste, I. Pastoriza-Santos, L.M. Liz-Marzán, P. Mulvaney, Gold nanorods: synthesis, characterization and applications, Coord. Chem. Rev. 249 (17) (2005) 1870−1901, https://doi.org/10.1016/j.ccr.2005.01.030.
[38] K.M. Mayer, S. Lee, H. Liao, B.C. Rostro, A. Fuentes, P.T. Scully, C.L. Nehl, J.H. Hafner, A label-free immunoassay based upon localized surface plasmon resonance of gold nanorods, ACS Nano 2 (4) (2008) 687−692, https://doi.org/10.1021/nn7003734.
[39] P. Senthil Kumar, I. Pastoriza-Santos, B. Rodríguez-González, F. Javier García de Abajo, L.M. Liz-Marzán, High-yield synthesis and optical response of gold nanostars, Nanotechnology 19 (1) (2007) 15606, https://doi.org/10.1088/0957-4484/19/01/015606.
[40] C.G. Khoury, T. Vo-Dinh, Gold nanostars for surface-enhanced Raman scattering: synthesis, characterization and optimization, J. Phys. Chem. C 112 (48) (2008) 18849−18859, https://doi.org/10.1021/jp8054747.
[41] C.L. Nehl, H. Liao, J.H. Hafner, Optical properties of star-shaped gold nanoparticles, Nano Lett. 6 (4) (2006) 683−688, https://doi.org/10.1021/nl052409y.

[42] F. Liebig, R. Henning, R.M. Sarhan, C. Prietzel, C.N.Z. Schmitt, M. Bargheer, J. Koetz, A simple one-step procedure to synthesise gold nanostars in concentrated aqueous surfactant solutions, RSC Adv. 9 (41) (2019) 23633−23641, https://doi.org/10.1039/C9RA02384D.

[43] H.S. Zhou, I. Honma, H. Komiyama, J.W. Haus, Controlled synthesis and quantum-size effect in gold-coated nanoparticles, Phys. Rev. B 50 (16) (1994) 12052−12056, https://doi.org/10.1103/PhysRevB.50.12052.

[44] T. Pham, J.B. Jackson, N.J. Halas, T.R. Lee, Preparation and characterization of gold nanoshells coated with self-assembled monolayers, Langmuir 18 (12) (2002) 4915−4920, https://doi.org/10.1021/la015561y.

[45] J. Turkevich, P.C. Stevenson, J. Hillier, A study of the nucleation and growth processes in the synthesis of colloidal gold, Discuss. Faraday Soc. 11 (0) (1951) 55−75, https://doi.org/10.1039/DF9511100055.

[46] J. Turkevich, Colloidal gold. part I, Gold Bull. 18 (3) (1985) 86−91, https://doi.org/10.1007/BF03214690.

[47] J. Kimling, M. Maier, B. Okenve, V. Kotaidis, H. Ballot, A. Plech, Turkevich method for gold nanoparticle synthesis revisited, J. Phys. Chem. B 110 (32) (2006) 15700−15707, https://doi.org/10.1021/jp061667w.

[48] N.R. Jana, L. Gearheart, C.J. Murphy, Wet chemical synthesis of high aspect ratio cylindrical gold nanorods, J. Phys. Chem. B 105 (19) (2001) 4065−4067, https://doi.org/10.1021/jp0107964.

[49] Y. Huang, W. Wang, H. Liang, H. Xu, Surfactant-Promoted reductive synthesis of shape-controlled gold nanostructures, Cryst. Growth Des. 9 (2) (2009) 858−862, https://doi.org/10.1021/cg800500c.

[50] N.D. Burrows, S. Harvey, F.A. Idesis, C.J. Murphy, Understanding the seed-mediated growth of gold nanorods through a fractional factorial design of experiments, Langmuir 33 (8) (2017) 1891−1907, https://doi.org/10.1021/acs.langmuir.6b03606.

[51] M. Chen, Y.-G. Feng, X. Wang, T.-C. Li, J.-Y. Zhang, D.-J. Qian, Silver nanoparticles capped by oleylamine: formation, growth, and self-organization, Langmuir 23 (10) (2007) 5296−5304, https://doi.org/10.1021/la700553d.

[52] N.J. Halas, S. Lal, W. Chang, S. Link, P. Nordlander, Plasmons in strongly coupled metallic nanostructures, Chem. Rev. 111 (2011) 3913.

[53] W. Stöber, A. Fink, E. Bohn, Controlled growth of monodisperse silica spheres in the micron size range, J. Colloid Interface Sci. 26 (1) (1968) 62−69, https://doi.org/10.1016/0021-9797(68)90272-5.

[54] N.R. Jana, L. Gearheart, C.J. Murphy, Wet chemical synthesis of silver nanorods and nanowires of controllable aspect ratio, Chem. Commun. (7) (2001) 617−618, https://doi.org/10.1039/B100521I.

[55] A.W. Orbaek, M.M. McHale, A.R. Barron, Synthesis and characterization of silver nanoparticles for an undergraduate laboratory, J. Chem. Educ. 92 (2) (2015) 339−344, https://doi.org/10.1021/ed500036b.

[56] X. Huang, I.H. El-Sayed, W. Qian, M.A. El-Sayed, Cancer cell imaging and photothermal therapy in the near-infrared region by using gold nanorods, J. Am. Chem. Soc. 128 (6) (2006) 2115−2120, https://doi.org/10.1021/ja057254a.

[57] J.J. Mock, M. Barbic, D.R. Smith, D.A. Schultz, S. Schultz, Shape effects in plasmon resonance of individual colloidal silver nanoparticles, J. Chem. Phys. 116 (15) (2002) 6755−6759, https://doi.org/10.1063/1.1462610.

[58] I. Pastoriza-Santos, D.S. Koktysh, A.A. Mamedov, M. Giersig, N.A. Kotov, L.M. Liz-Marzán, One-pot synthesis of Ag@TiO_2 core−shell nanoparticles and their layer-by-layer assembly, Langmuir 16 (6) (2000) 2731−2735, https://doi.org/10.1021/la991212g.

[59] H. Sakai, T. Kanda, H. Shibata, T. Ohkubo, M. Abe, Preparation of highly dispersed core/shell-type titania nanocapsules containing a single Ag nanoparticle, J. Am. Chem. Soc. 128 (15) (2006) 4944−4945, https://doi.org/10.1021/ja058083c.

[60] K.S. Mayya, D.I. Gittins, F. Caruso, Gold−titania core−shell nanoparticles by polyelectrolyte complexation with a titania precursor, Chem. Mater. 13 (11) (2001) 3833−3836, https://doi.org/10.1021/cm011128y.

[61] F. Caruso, Nanoengineering of particle surfaces, Adv. Mater. 13 (1) (2001) 11–22, https://doi.org/10.1002/1521-4095(200101)13:1<11::AID-ADMA11>3.0.CO;2-N.

[62] N. Zhang, S. Liu, X. Fu, Y.-J. Xu, Synthesis of M@TiO_2 (M = Au, Pd, Pt) core–shell nanocomposites with tunable photoreactivity, J. Phys. Chem. C 115 (18) (2011) 9136–9145, https://doi.org/10.1021/jp2009989.

[63] Y.-C. Pu, G. Wang, K.-D. Chang, Y. Ling, Y.-K. Lin, B.C. Fitzmorris, C.-M. Liu, X. Lu, Y. Tong, J.Z. Zhang, Y.-J. Hsu, Y. Li, Au nanostructure-decorated TiO_2 nanowires exhibiting photoactivity across entire UV-visible region for photoelectrochemical water splitting, Nano Lett. 13 (8) (2013) 3817–3823, https://doi.org/10.1021/nl4018385.

[64] Z. Zhang, Z. Wang, S.-W. Cao, C. Xue, Au/Pt nanoparticle-decorated TiO_2 nanofibers with plasmon-enhanced photocatalytic activities for solar-to-fuel conversion, J. Phys. Chem. C 117 (49) (2013) 25939–25947, https://doi.org/10.1021/jp409311x.

[65] D.D. Lekeufack, A. Brioude, A. Mouti, J.G. Alauzun, P. Stadelmann, A.W. Coleman, P. Miele, Core–shell Au@(TiO_2, SiO_2) nanoparticles with tunable morphology, Chem. Commun. 46 (25) (2010) 4544–4546, https://doi.org/10.1039/C0CC00935K.

[66] R. Malik, V. Chaudhary, V.K. Tomer, P.S. Rana, S.P. Nehra, S. Duhan, Visible light-driven mesoporous Au–TiO_2/SiO_2 photocatalysts for advanced oxidation process, Ceram. Int. 42 (9) (2016) 10892–10901, https://doi.org/10.1016/j.ceramint.2016.03.222.

[67] S. Yuyang, J. Long, Z. Tian, W. Jin, L. Ling, J. Yong, J. Zhifeng, S. Xiaosong, Synthesis of Au–ZnO hybrid nanostructure arrays and their enhanced photocatalytic activity, New J. Chem. 39 (4) (2015) 2943–2948, https://doi.org/10.1039/C5NJ00124B.

[68] E.J. Guidelli, O. Baffa, D.R. Clarke, Enhanced UV emission from silver/ZnO And gold/ZnO core-shell nanoparticles: photoluminescence, radioluminescence, and optically stimulated luminescence, Sci. Rep. 5 (1) (2015) 14004, https://doi.org/10.1038/srep14004.

[69] S. Chu, J. Ren, D. Yan, J. Huang, J. Liu, Noble metal nanodisks epitaxially formed on ZnO nanorods and their effect on photoluminescence, Appl. Phys. Lett. 101 (4) (2012) 43122, https://doi.org/10.1063/1.4739516.

[70] C.W. Cheng, E.J. Sie, B. Liu, C.H.A. Huan, T.C. Sum, H.D. Sun, H.J. Fan, Surface plasmon enhanced band edge luminescence of ZnO nanorods by capping Au nanoparticles, Appl. Phys. Lett. 96 (7) (2010) 71107, https://doi.org/10.1063/1.3323091.

[71] M. Mahanti, D. Basak, Highly enhanced UV emission due to surface plasmon resonance in Ag–ZnO nanorods, Chem. Phys. Lett. 542 (2012) 110–116, https://doi.org/10.1016/j.cplett.2012.06.004.

[72] N. Zhang, W. Tang, P. Wang, X. Zhang, Z. Zhao, In situ enhancement of NBE emission of Au–ZnO composite nanowires by SPR, CrystEngComm 15 (17) (2013) 3301–3304, https://doi.org/10.1039/C3CE40114F.

[73] X. Li, Y. Zhang, X. Ren, Effects of localized surface plasmons on the photoluminescence properties of Au-coated ZnO films, Optic Express 17 (11) (2009) 8735–8740, https://doi.org/10.1364/OE.17.008735.

[74] N. Gogurla, A.K. Sinha, S. Santra, S. Manna, S.K. Ray, Multifunctional Au-ZnO plasmonic nanostructures for enhanced UV photodetector and room temperature NO sensing devices, Sci. Rep. 4 (1) (2014) 6483, https://doi.org/10.1038/srep06483.

[75] R.H. Kodama, Magnetic nanoparticles, J. Magn. Magn Mater. 200 (1) (1999) 359–372, https://doi.org/10.1016/S0304-8853(99)00347-9.

[76] S.R. Dave, X. Gao, Monodisperse magnetic nanoparticles for biodetection, imaging, and drug delivery: a versatile and evolving technology, WIREs Nanomed. Nanobiotechnol. 1 (6) (2009) 583–609, https://doi.org/10.1002/wnan.51.

[77] H. Gu, K. Xu, C. Xu, B. Xu, Biofunctional magnetic nanoparticles for protein separation and pathogen detection, Chem. Commun. (9) (2006) 941–949, https://doi.org/10.1039/B514130C.

[78] J.R. McCarthy, K.A. Kelly, E.Y. Sun, R. Weissleder, Targeted delivery of multifunctional magnetic nanoparticles, Nanomedicine 2 (2) (2007) 153–167, https://doi.org/10.2217/17435889.2.2.153.

[79] S. Peng, C. Lei, Y. Ren, R.E. Cook, Y. Sun, Plasmonic/magnetic bifunctional nanoparticles, Angew. Chem. Int. Ed. 50 (14) (2011) 3158−3163, https://doi.org/10.1002/anie.201007794.

[80] S.K. Yen, P. Padmanabhan, S.T. Selvan, Multifunctional iron oxide nanoparticles for diagnostics, therapy and macromolecule delivery, Theranostics 3 (12) (2013) 986−1003, https://doi.org/10.7150/thno.4827.

[81] A. Akbarzadeh, M. Samiei, S. Davaran, Magnetic nanoparticles: preparation, physical properties, and applications in biomedicine, Nanoscale Res. Lett. 7 (1) (2012) 144, https://doi.org/10.1186/1556-276X-7-144.

[82] R. Bardhan, S. Lal, A. Joshi, N.J. Halas, Theranostic nanoshells: from probe design to imaging and treatment of cancer, Acc. Chem. Res. 44 (10) (2011) 936−946, https://doi.org/10.1021/ar200023x.

[83] J. Zhao, M. Wallace, M.P. Melancon, Cancer theranostics with gold nanoshells, Nanomedicine 9 (13) (2014) 2041−2057, https://doi.org/10.2217/nnm.14.136.

[84] C.S. Levin, C. Hofmann, T.A. Ali, A.T. Kelly, E. Morosan, P. Nordlander, K.H. Whitmire, N.J. Halas, Magnetic−plasmonic core−shell nanoparticles, ACS Nano 3 (6) (2009) 1379−1388, https://doi.org/10.1021/nn900118a.

[85] E. Prodan, C. Radloff, N.J. Halas, P. Nordlander, A hybridization model for the plasmon response of complex nanostructures, Science 302 (5644) (2003), https://doi.org/10.1126/science.1089171, 419 LP − 422.

[86] J. Gao, H. Gu, B. Xu, Multifunctional magnetic nanoparticles: design, synthesis, and biomedical applications, Acc. Chem. Res. 42 (8) (2009) 1097−1107, https://doi.org/10.1021/ar9000026.

[87] M. Mahmoudi, H. Hosseinkhani, M. Hosseinkhani, S. Boutry, A. Simchi, W.S. Journeay, K. Subramani, S. Laurent, Magnetic resonance imaging tracking of stem cells in vivo using iron oxide nanoparticles as a tool for the advancement of clinical regenerative medicine, Chem. Rev. 111 (2) (2011) 253−280, https://doi.org/10.1021/cr1001832.

[88] M. Mahmoudi, S. Sant, B. Wang, S. Laurent, T. Sen, Superparamagnetic iron oxide nanoparticles (SPIONs): development, surface modification and applications in chemotherapy, Adv. Drug Deliv. Rev. 63 (1) (2011) 24−46, https://doi.org/10.1016/j.addr.2010.05.006.

[89] K.R. Wierzbinski, T. Szymanski, N. Rozwadowska, J.D. Rybka, A. Zimna, T. Zalewski, K. Nowicka-Bauer, A. Malcher, M. Nowaczyk, M. Krupinski, M. Fiedorowicz, P. Bogorodzki, P. Grieb, M. Giersig, M.K. Kurpisz, Potential use of superparamagnetic iron oxide nanoparticles for in vitro and in vivo bioimaging of human myoblasts, Sci. Rep. 8 (1) (2018) 3682, https://doi.org/10.1038/s41598-018-22018-0.

[90] E.V. Shevchenko, M.I. Bodnarchuk, M.V. Kovalenko, D.V. Talapin, R.K. Smith, S. Aloni, W. Heiss, A.P. Alivisatos, gold/iron oxide core/hollow-shell nanoparticles, Adv. Mater. 20 (22) (2008) 4323−4329, https://doi.org/10.1002/adma.200702994.

[91] L. León Félix, J.A.H. Coaquira, M.A.R. Martínez, G.F. Goya, J. Mantilla, M.H. Sousa, L. Valladares, S. de los, C.H.W. Barnes, P.C. Morais, Structural and magnetic properties of core-shell Au/Fe_3O_4 nanoparticles, Sci. Rep. 7 (1) (2017) 41732, https://doi.org/10.1038/srep41732.

[92] M. Abbas, S. RamuluTorati, C. Kim, Multifunctional Fe_3O_4/Au core/satellite nanocubes: an efficient chemical synthesis, characterization and functionalization of streptavidin protein, Dalton Trans. 46 (7) (2017) 2303−2309, https://doi.org/10.1039/C6DT04486G.

[93] X. Zhou, W. Xu, Y. Wang, Q. Kuang, Y. Shi, L. Zhong, Q. Zhang, Fabrication of cluster/shell Fe_3O_4/Au nanoparticles and application in protein detection via a SERS method, J. Phys. Chem. C 114 (46) (2010) 19607−19613, https://doi.org/10.1021/jp106949v.

[94] L. León Félix, B. Sanz, V. Sebastián, T.E. Torres, M.H. Sousa, J.A.H. Coaquira, M.R. Ibarra, G.F. Goya, Gold-decorated magnetic nanoparticles design for hyperthermia applications and as a potential platform for their surface-functionalization, Sci. Rep. 9 (1) (2019) 4185, https://doi.org/10.1038/s41598-019-40769-2.

[95] F. Bao, J.-L. Yao, R.-A. Gu, Synthesis of magnetic Fe_2O_3/Au core/shell nanoparticles for bioseparation and immunoassay based on surface-enhanced raman spectroscopy, Langmuir 25 (18) (2009) 10782−10787, https://doi.org/10.1021/la901337r.

[96] Z. Xu, Y. Hou, S. Sun, Magnetic core/shell Fe_3O_4/Au and Fe_3O_4/Au/Ag nanoparticles with tunable plasmonic properties, J. Am. Chem. Soc. 129 (28) (2007) 8698–8699, https://doi.org/10.1021/ja073057v.

[97] S.I. Stoeva, F. Huo, J.-S. Lee, C.A. Mirkin, Three-layer composite magnetic nanoparticle probes for DNA, J. Am. Chem. Soc. 127 (44) (2005) 15362–15363, https://doi.org/10.1021/ja055056d.

[98] M. Nakamura, K. Katagiri, K. Koumoto, Preparation of hybrid hollow capsules formed with Fe_3O_4 and polyelectrolytes via the layer-by-layer assembly and the aqueous solution process, J. Colloid Interface Sci. 341 (1) (2010) 64–68, https://doi.org/10.1016/j.jcis.2009.09.014.

[99] Y. Hu, L. Meng, L. Niu, Q. Lu, Facile synthesis of superparamagnetic Fe_3O_4@polyphosphazene@Au shells for magnetic resonance imaging and photothermal therapy, ACS Appl. Mater. Interfaces 5 (11) (2013) 4586–4591, https://doi.org/10.1021/am400843d.

[100] B. Liu, W. Zhang, F. Yang, H. Feng, X. Yang, Facile method for synthesis of Fe_3O_4@polymer microspheres and their application as magnetic support for loading metal nanoparticles, J. Phys. Chem. C 115 (32) (2011) 15875–15884, https://doi.org/10.1021/jp204976y.

[101] I. Monaco, F. Arena, S. Biffi, E. Locatelli, B. Bortot, F. La Cava, G.M. Marini, G.M. Severini, E. Terreno, M. Comes Franchini, Synthesis of lipophilic core–shell Fe_3O_4@SiO_2@Au nanoparticles and polymeric entrapment into nanomicelles: a novel nanosystem for in vivo active targeting and magnetic resonance–photoacoustic dual imaging, Bioconjugate Chem. 28 (5) (2017) 1382–1390, https://doi.org/10.1021/acs.bioconjchem.7b00076.

[102] E.A. Kwizera, E. Chaffin, X. Shen, J. Chen, Q. Zou, Z. Wu, Z. Gai, S. Bhana, R. O'Connor, L. Wang, H. Adhikari, S.R. Mishra, Y. Wang, X. Huang, Size- and shape-controlled synthesis and properties of magnetic–plasmonic core–shell nanoparticles, J. Phys. Chem. C 120 (19) (2016) 10530–10546, https://doi.org/10.1021/acs.jpcc.6b00875.

[103] S.-J. Cho, J.-C. Idrobo, J. Olamit, K. Liu, N.D. Browning, S.M. Kauzlarich, Growth mechanisms and oxidation resistance of gold-coated iron nanoparticles, Chem. Mater. 17 (12) (2005) 3181–3186, https://doi.org/10.1021/cm0500713.

[104] J. Reguera, D. Jiménez de Aberasturi, M. Henriksen-Lacey, J. Langer, A. Espinosa, B. Szczupak, C. Wilhelm, L.M. Liz-Marzán, Janus plasmonic–magnetic gold–iron oxide nanoparticles as contrast agents for multimodal imaging, nanoscale 9 (27) (2017) 9467–9480, https://doi.org/10.1039/C7NR01406F.

[105] C. Gong, Q. Li, H. Zhou, R. Liu, Tiny Au satellites decorated Fe_3O_4@3-aminophenol-formaldehyde core-shell nanoparticles: easy synthesis and comparison in catalytic reduction for cationic and anionic dyes, Colloids Surfaces A Physicochem. Eng. Asp. 540 (2018) 67–72, https://doi.org/https://doi.org/10.1016/j.colsurfa.2017.12.045.

[106] G.A. Sotiriou, A.M. Hirt, P.-Y. Lozach, A. Teleki, F. Krumeich, S.E. Pratsinis, Hybrid, silica-coated, janus-like plasmonic-magnetic nanoparticles, Chem. Mater. 23 (7) (2011) 1985–1992, https://doi.org/10.1021/cm200399t.

[107] H. Gu, Z. Yang, J. Gao, C.K. Chang, B. Xu, Heterodimers of nanoparticles: formation at a liquid–liquid interface and particle-specific surface modification by functional molecules, J. Am. Chem. Soc. 127 (1) (2005) 34–35, https://doi.org/10.1021/ja045220h.

[108] H. Yu, M. Chen, P.M. Rice, S.X. Wang, R.L. White, S. Sun, Dumbbell-like bifunctional Au–Fe_3O_4 nanoparticles, Nano Lett. 5 (2) (2005) 379–382, https://doi.org/10.1021/nl047955q.

[109] C. Langlois, P. Benzo, R. Arenal, M. Benoit, J. Nicolai, N. Combe, A. Ponchet, M.J. Casanove, Fully crystalline faceted Fe–Au core–shell nanoparticles, Nano Lett. 15 (8) (2015) 5075–5080, https://doi.org/10.1021/acs.nanolett.5b02273.

[110] C. Xu, B. Wang, S. Sun, Dumbbell-like Au–Fe_3O_4 nanoparticles for target-specific platin delivery, J. Am. Chem. Soc. 131 (12) (2009) 4216–4217, https://doi.org/10.1021/ja900790v.

[111] A. La Porta, A. Sánchez-Iglesias, T. Altantzis, S. Bals, M. Grzelczak, L.M. Liz-Marzán, Multifunctional self-assembled composite colloids and their application to SERS detection, Nanoscale 7 (23) (2015) 10377–10381, https://doi.org/10.1039/C5NR01264C.

[112] V. Amendola, S. Scaramuzza, L. Litti, M. Meneghetti, G. Zuccolotto, A. Rosato, E. Nicolato, P. Marzola, G. Fracasso, C. Anselmi, M. Pinto, M. Colombatti, Magneto-plasmonic Au-Fe alloy nanoparticles designed for multimodal SERS-MRI-CT imaging, Small 10 (12) (2014) 2476−2486, https://doi.org/10.1002/smll.201303372.

[113] G. Sharma, P.A. Jeevanandam, Facile synthesis of multifunctional iron oxide@Ag core−shell nanoparticles and their catalytic applications, Eur. J. Inorg. Chem. 2013 (36) (2013) 6126−6136, https://doi.org/10.1002/ejic.201301193.

[114] S. Scaramuzza, D. Badocco, P. Pastore, D.F. Coral, M.B. Fernández van Raap, V. Amendola, Magnetically assembled SERS substrates composed of iron−silver nanoparticles obtained by laser ablation in liquid, ChemPhysChem 18 (9) (2017) 1026−1034, https://doi.org/10.1002/cphc.201600651.

[115] S. Chang, W. Yun, S.L. Eichmann, M.E. Poitzsch, W. Wang, Magnetic SERS composite nanoparticles for microfluidic oil reservoir tracer detection and nanoprobe applications, ACS Appl. Nano Mater. 2 (2) (2019) 997−1004, https://doi.org/10.1021/acsanm.8b02291.

[116] R. Weissleder, G. Elizondo, J. Wittenberg, C.A. Rabito, H.H. Bengele, L. Josephson, Ultrasmall superparamagnetic iron oxide: characterization of a new class of contrast agents for MR imaging, Radiology 175 (2) (1990) 489−493, https://doi.org/10.1148/radiology.175.2.2326474.

[117] J. Xie, G. Liu, H.S. Eden, H. Ai, X. Chen, Surface-engineered magnetic nanoparticle platforms for cancer imaging and therapy, Acc. Chem. Res. 44 (10) (2011) 883−892, https://doi.org/10.1021/ar200044b.

[118] T.A. Larson, J. Bankson, J. Aaron, K. Sokolov, Hybrid plasmonic magnetic nanoparticles as molecular specific agents for MRI/optical imaging and photothermal therapy of cancer cells, Nanotechnology 18 (32) (2007) 325101, https://doi.org/10.1088/0957-4484/18/32/325101.

[119] R. Bardhan, W. Chen, C. Perez-Torres, M. Bartels, R.M. Huschka, L.L. Zhao, E. Morosan, R.G. Pautler, A. Joshi, N.J. Halas, Nanoshells with targeted simultaneous enhancement of magnetic and optical imaging and photothermal therapeutic response, Adv. Funct. Mater. 19 (24) (2009) 3901−3909, https://doi.org/10.1002/adfm.200901235.

[120] Z. Fan, M. Shelton, A.K. Singh, D. Senapati, S.A. Khan, P.C. Ray, Multifunctional plasmonic shell−magnetic core nanoparticles for targeted diagnostics, isolation, and photothermal destruction of tumor cells, ACS Nano 6 (2) (2012) 1065−1073, https://doi.org/10.1021/nn2045246.

[121] J. Yao, M. Yang, Y. Duan, Chemistry, biology, and medicine of fluorescent nanomaterials and related systems: new insights into biosensing, bioimaging, genomics, diagnostics, and therapy, Chem. Rev. 114 (12) (2014) 6130−6178, https://doi.org/10.1021/cr200359p.

[122] O. Akturk, O. Erdemli, B.C. Tunali, in: V. Grumezescu, A.M.B. Grumezescu (Eds.), Chapter 15 - Gold Nanocomposites for Biomedical Applications, Elsevier, 2019, pp. 485−525, https://doi.org/10.1016/B978-0-12-818431-8.00015-5.

[123] N.C. Bigall, W.J. Parak, D. Dorfs, Fluorescent, magnetic and plasmonic—hybrid multifunctional colloidal nano objects, Nano Today 7 (4) (2012) 282−296, https://doi.org/10.1016/j.nantod.2012.06.007.

[124] G.A. Sotiriou, Biomedical applications of multifunctional plasmonic nanoparticles, WIREs Nanomed. Nanobiotechnol. 5 (1) (2013) 19−30, https://doi.org/10.1002/wnan.1190.

[125] Y. Wang, B. Yan, L. Chen, SERS tags: novel optical nanoprobes for bioanalysis, Chem. Rev. 113 (3) (2013) 1391−1428, https://doi.org/10.1021/cr300120g.

[126] J. Shen, Y. Zhu, X. Yang, J. Zong, C. Li, Multifunctional Fe_3O_4@Ag/SiO_2/Au core−shell microspheres as a novel SERS-activity label via long-range plasmon coupling, Langmuir 29 (2) (2013) 690−695, https://doi.org/10.1021/la304048v.

[127] K.C.-F. Leung, S. Xuan, X. Zhu, D. Wang, C.-P. Chak, S.-F. Lee, W.K.-W. Ho, B.C.-T. Chung, Gold and iron oxide hybrid nanocomposite materials, Chem. Soc. Rev. 41 (5) (2012) 1911−1928, https://doi.org/10.1039/C1CS15213K.

[128] T. Udayabhaskararao, Y. Sun, N. Goswami, S.K. Pal, K. Balasubramanian, T. Pradeep, Ag7Au6: A 13-atom alloy quantum cluster, Angew. Chem. Int. Ed. 51 (9) (2012) 2155−2159, https://doi.org/10.1002/anie.201107696.

[129] J. Zheng, J.T. Petty, R.M. Dickson, High quantum yield blue emission from water-soluble Au8 nanodots, J. Am. Chem. Soc. 125 (26) (2003) 7780–7781, https://doi.org/10.1021/ja035473v.

[130] J. Zheng, C. Zhang, R.M. Dickson, Highly fluorescent, water-soluble, size-tunable gold quantum dots, Phys. Rev. Lett. 93 (7) (2004) 77402, https://doi.org/10.1103/PhysRevLett.93.077402.

[131] R. Jin, Quantum sized, thiolate-protected gold nanoclusters, Nanoscale 2 (3) (2010) 343–362, https://doi.org/10.1039/B9NR00160C.

[132] O. Kulakovich, N. Strekal, A. Yaroshevich, S. Maskevich, S. Gaponenko, I. Nabiev, U. Woggon, M. Artemyev, Enhanced luminescence of CdSe quantum dots on gold colloids, Nano Lett. 2 (12) (2002) 1449–1452, https://doi.org/10.1021/nl025819k.

[133] H. Chen, T. Ming, L. Zhao, F. Wang, L.-D. Sun, J. Wang, C.-H. Yan, Plasmon–molecule interactions, Nano Today 5 (5) (2010) 494–505, https://doi.org/10.1016/j.nantod.2010.08.009.

[134] Y. Jin, X. Gao, Plasmonic fluorescent quantum dots, Nat. Nanotechnol. 4 (9) (2009) 571–576, https://doi.org/10.1038/nnano.2009.193.

[135] B. Ji, E. Giovanelli, B. Habert, P. Spinicelli, M. Nasilowski, X. Xu, N. Lequeux, J.-P. Hugonin, F. Marquier, J.-J. Greffet, B. Dubertret, Non-blinking quantum dot with a plasmonic nanoshell resonator, Nat. Nanotechnol. 10 (2) (2015) 170–175, https://doi.org/10.1038/nnano.2014.298.

[136] F. Song, P.S. Tang, H. Durst, D.T. Cramb, W.C.W. Chan, Nonblinking plasmonic quantum dot assemblies for multiplex biological detection, Angew. Chem. Int. Ed. 51 (35) (2012) 8773–8777, https://doi.org/10.1002/anie.201201872.

[137] E. Cohen-Hoshen, G.W. Bryant, I. Pinkas, J. Sperling, I. Bar-Joseph, Exciton–plasmon interactions in quantum dot–gold nanoparticle structures, Nano Lett. 12 (8) (2012) 4260–4264, https://doi.org/10.1021/nl301917d.

[138] K.S. Novoselov, V.I. Fal'ko, L. Colombo, P.R. Gellert, M.G. Schwab, K. Kim, A roadmap for graphene, Nature 490 (2012) 192.

[139] X. Huang, X. Qi, F. Boey, H. Zhang, Graphene-based composites, Chem. Soc. Rev. 41 (2) (2012) 666–686, https://doi.org/10.1039/C1CS15078B.

[140] W. Xu, N. Mao, J. Zhang, Graphene: a platform for surface-enhanced raman spectroscopy, Small 9 (8) (2013) 1206–1224, https://doi.org/10.1002/smll.201203097.

[141] X. Yu, H. Cai, W. Zhang, X. Li, N. Pan, Y. Luo, X. Wang, J.G. Hou, Tuning chemical enhancement of SERS by controlling the chemical reduction of graphene oxide nanosheets, ACS Nano 5 (2) (2011) 952–958, https://doi.org/10.1021/nn102291j.

[142] G. Goncalves, P.A.A.P. Marques, C.M. Granadeiro, H.I.S. Nogueira, M.K. Singh, J. Grácio, Surface modification of graphene nanosheets with gold nanoparticles: the role of oxygen moieties at graphene surface on gold nucleation and growth, Chem. Mater. 21 (20) (2009) 4796–4802, https://doi.org/10.1021/cm901052s.

[143] Y.-K. Kim, H.-K. Na, Y.W. Lee, H. Jang, S.W. Han, D.-H. Min, The direct growth of gold rods on graphene thin films, Chem. Commun. 46 (18) (2010) 3185–3187, https://doi.org/10.1039/C002002H.

[144] K. Turcheniuk, R. Boukherroub, S. Szunerits, Gold–graphene nanocomposites for sensing and biomedical applications, J. Mater. Chem. B 3 (21) (2015) 4301–4324, https://doi.org/10.1039/C5TB00511F.

[145] Y. Wang, L. Polavarapu, L.M. Liz-Marzán, Reduced graphene oxide-supported gold nanostars for improved SERS sensing and drug delivery, ACS Appl. Mater. Interfaces 6 (24) (2014) 21798–21805, https://doi.org/10.1021/am501382y.

[146] S.K. Bhunia, N.R. Jana, Reduced graphene oxide-silver nanoparticle composite as visible light photocatalyst for degradation of colorless endocrine disruptors, ACS Appl. Mater. Interfaces 6 (22) (2014) 20085–20092, https://doi.org/10.1021/am505677x.

[147] C. Hu, Y. Liu, J. Qin, G. Nie, B. Lei, Y. Xiao, M. Zheng, J. Rong, Fabrication of reduced graphene oxide and silver nanoparticle hybrids for raman detection of absorbed folic acid: a potential cancer diagnostic probe, ACS Appl. Mater. Interfaces 5 (11) (2013) 4760–4768, https://doi.org/10.1021/am4000485.

[148] S.Z. Nergiz, N. Gandra, S. Singamaneni, Self-assembled high aspect ratio gold nanostar/graphene oxide hybrid nanorolls, Carbon 66 (2014) 585–591, https://doi.org/10.1016/j.carbon.2013.09.042.

[149] A.K. Nair, K.M. Sukumaran Nair, S. Thomas, D. Rouxel, S. Alwarappan, N. Kalarikkal, In situ synthesis of silver nanospheres, nanocubes, and nanowires over boron-doped graphene sheets for surface-enhanced raman scattering application and enzyme-free detection of hydrogen peroxide, Langmuir 34 (45) (2018) 13603–13614, https://doi.org/10.1021/acs.langmuir.8b02005.

[150] J. Li, C. Liu, Ag/graphene heterostructures: synthesis, characterization and optical properties, Eur. J. Inorg. Chem. 2010 (8) (2010) 1244–1248, https://doi.org/10.1002/ejic.200901048.

[151] T. Demeritte, B.P. Viraka Nellore, R. Kanchanapally, S.S. Sinha, A. Pramanik, S.R. Chavva, P.C. Ray, Hybrid graphene oxide based plasmonic-magnetic multifunctional nanoplatform for selective separation and label-free identification of alzheimer's disease biomarkers, ACS Appl. Mater. Interfaces 7 (24) (2015) 13693–13700, https://doi.org/10.1021/acsami.5b03619.

[152] Y. Hu, Á.I. López-Lorente, B. Mizaikoff, Graphene-based surface enhanced vibrational spectroscopy: recent developments, challenges, and applications, ACS Photonics 6 (9) (2019) 2182–2197, https://doi.org/10.1021/acsphotonics.9b00645.

[153] Y. Feng, Q. Chen, Q. Yin, G. Pan, Z. Tu, L. Liu, Reduced graphene oxide functionalized with gold nanostar nanocomposites for synergistically killing bacteria through intrinsic antimicrobial activity and photothermal ablation, ACS Appl. Bio Mater. 2 (2) (2019) 747–756, https://doi.org/10.1021/acsabm.8b00608.

[154] B. Chandu, C.M. Kurmarayuni, S. Kurapati, H.B. Bollikolla, Green and economical synthesis of graphene–silver nanocomposite exhibiting excellent photocatalytic efficiency, Carbon Lett. 30 (2) (2020) 225–233, https://doi.org/10.1007/s42823-019-00091-3.

[155] R. Suresh, R.V. Mangalaraja, H.D. Mansilla, P. Santander, J. Yáñez, in: M. Naushad, S. Rajendran, E. Lichtfouse (Eds.), Reduced Graphene Oxide-Based Photocatalysis BT - Green Photocatalysts, Springer International Publishing, Cham, 2020, pp. 145–166, https://doi.org/10.1007/978-3-030-15608-4_6.

[156] P.B. Jimenez-Vara, J. Johny, I.C. Novoa-de Leon, C. Guerrero-Bermea, D.F. Garcia-Gutierrez, D.I. Garcia-Gutierrez, L. Chavez-Guerrero, S. Sepulveda-Guzman, Hybrid films of reduced graphene oxide modified with gold nanorods and its study as surface-enhanced raman spectroscopy platform, Mater. Lett. 265 (2020) 127405, https://doi.org/10.1016/j.matlet.2020.127405.

[157] Praveenkumar Pinapati, Jostine Puthenveetil Joby, Sudhir Cherukulappurath, Graphene Oxide Based Two-Dimensional Optical Tweezers for Low Power Trapping of Quantum Dots and *E. coli* Bacteria, ACS Appl. Nano Mater. 3 (6) (2020) 5107–5115, https://doi.org/10.1021/acsanm.0c00367.